

MIDI Optical Path Differences and Phases

Richard J. Mathar*

Sterrewacht Leiden, P.O. Box 9513, 2300 RA Leiden, The Netherlands

(Dated: June 25, 2009)

Although the terminology of optical path differences in the VLTI nomenclature is concealed by an almost arbitrary reference to some beam enumeration in the VLTI laboratory, the FITS tables produced by the VLTI/MIDI interferometer contain all the information to interpret the motions of the internal and main delay line mirrors unambiguously. The text is arranged in a “Q&A” fashion.

Updates of this text are placed on

<http://www.strw.leidenuniv.nl/~mathar/public/matharMIDI20051110.pdf>.

Contents

I. OPD Information Encoded in MIDI FITS Files	2
A. Which of the two piezos (internal delay lines) moved?	2
B. What is the MIDI OPD sign convention?	3
C. Which of the two telescopes was closer to the star?	4
D. Which of the two telescopes collected beam A, which beam B?	5
E. Was the OPL of beam A longer than the OPL of beam B?	5
F. Did the MDL passed by beam A or the one passed by beam B move?	5
G. What was the actual external OPD?	6
H. How do piezo movements relocate the point of ZOPD on the sky?	7
1. Qualitative: Sign	7
2. Quantitative	8
I. Phase measurements with MIDI	10
II. Imaging Information Encoded in MIDI FITS Files	12
A. Where is North in the VLTI beams?	12
1. Without DDL or STS	12
2. With DDL and/or STS	13
B. Where is North on the MIDI detector?	14
C. How does the baseline project onto the sky?	18
A. Baseline Azimuth Angles	18
B. Head files of split exposures	19
C. Pupil rotation in the VLTI train	20
D. Atmospheric N band transmission	22
E. Software Problem Reports	25
1. VLTSW20050024	25
2. VLTSW20050104	26
3. VLTSW20060050	26
4. VLTSW20060066	27
5. VLTSW20060227	31
F. Spheroidal Coordinates	32
G. Web Page Change Requests	32

*URL: <http://www.strw.leidenuniv.nl/~mathar>

1. WWW-31864	32
H. Acronyms	33
I. Notations	35
References	35

I. OPD INFORMATION ENCODED IN MIDI FITS FILES

A. Which of the two piezos (internal delay lines) moved?

1. The motions of the two piezo-driven internal delay lines are recorded in the LOCALOPD column of the IMAGING_DATA table. Simple inspection on a case by case reveals whether the numbers in LOCALOPD[1] associated with beam A, or the numbers in LOCALOPD[2] associated with beam B changed with time.

See again [18, 1.5.6] to disentangle the definition of beam A and beam B. Throughout this text here, I use the definition introduced by the consortium [12, 30, 32], where beam A is the western of the two beams that enter the optical table, the one that passes by the DLMT — which is the opposite of the nomenclature introduced later by ESO. The figure caption of [12, Fig. 1] is correct, but the description of the beam combiner reflection/transmission on page 2 of [12] should have the nomenclature swapped.

The 1-based indexing follows FITS rules; showing the data with a variety of programming languages may display them 0-based. One can actually create schedules which move both piezos at the same time as described in [18, 3.4], but the simplified interface offered through the templates to the standard observer ensures that only one of the two piezos is moving during the exposure.

If `fv` is installed, one can have an immediate look at this information with

```
fv your_file_name.fits
```

click on the button under the column All which selects the extension IMAGING_DATA. This opens a window with a table with columns FRAME, TIME, EXPTIME and so on up to INS_TRAIN. Now there are two ways to move on

- Click on the Tools button in the header of this new window and select Plot..., which opens another window. (This could also be reached by clicking Plot in the earlier window.) Enter either FRAME or TIME in the field Column name to the right of the X. Enter LOCALOPD[1] in the field Column name to the right of the Y. Click on Go, which shows the zig-zag pattern of the motions of piezo A. For comparison, close this POW window with File and CLOSE POW, and use again Tools and Plot..., this time with LOCALOPD[2] in the Y field. This will open a window with a graph that effectively appears blank because these values are zero and fall right on top of the axis of the plot. To get an impression of the combined OPD of the MDL and internal delay line, you may enter `OPD[2]+LOCALOPD[2]-OPD[1]-LOCALOPD[1]` into the Y field, which displays the arithmetic sum-difference between the corresponding columns.
 - Left-right scroll the table with the columns until one can click on the Modify underneath the LOCALOPD column. Select Expand which opens a new window with two columns. (With older fv versions, this is not needed and the two columns are already displayed both side by side.) If the left column shows negative numbers in the range of -1×10^{-5} (to be interpreted as meters) and the right column shows zeros, piezo A is moving; if the left column shows zeros and the right one negative numbers, piezo A was standing and piezo B was moving.
2. In addition, the same information is in the SCAN_SETUP1 binary table in each first of the split FITS files of an exposure (see App. B): only one of the LOC_OPL columns changes as a function of time, ie, along the table rows. A command like

```
dtfits MIDI.2005-05-27T09:50:29.250.fi* | tail -30
```

would reveal this information if the [eclipse](#) software has been installed on your computer. A faster way is running my `Fits2Ascii` available from

<http://www.strw.leidenuniv.nl/~mathar/progs/Ascii2Fits.C>, or interactive inspection with `fv`.

3. There is a statistical bias toward moving beam A to scan fringes. This is a mere result of having defaults in some templates which the ordinary P2PP user would hardly bother to change or would not even be offered to change; it does not guarantee that this will always be the case. In particular, to enhance the internal delay from the 150 μm of a single piezo to the combined total stroke of 300 μm if both are moved at the same time, the interface to the schedule builder within the OS [18] allows synchronized motions of both. The combination

“short FITS” SETUP keyword	value
INS PIEZ1 BASE1	0.
INS PIEZ1 STROKE1	$-150.e - 6$
INS PIEZ2 BASE1	$-150.e - 6$
INS PIEZ2 STROKE1	$+150.e - 6$
INS PIEZ POSNUM1	5

for example would start at positions with piezo(Beam A) adding maximum delay to Beam A and piezo(Beam B) adding minimum delay to Beam B, and both ending up after each scan (in 5 steps of $\pm 30 \mu\text{m}$ change in OPL per step per beam, combined 60 μm change in OPD per step) at the opposite extreme position. Of course one could start at an internal OPD which is different by 300 μm and flip the sign of the time-derivative of the OPD along the scan altogether by swapping the values between PIEZ1 and PIEZ2. The interface does not allow asynchronous motion, which means there is only one POSNUM value—without index at the PIEZ part of the keyword—that is used to create the motion schedules. (Detailed descriptions are in the CMM module dicMIDI which is accessible on the IWS and—not necessarily up-to-date—in <http://archive.eso.org/DICB> in the dictionary database link as ESO-VLT-DIC.MIDI.ICS.)

The pieces of information obtained from the first two items listed above ought be consistent.

B. What is the MIDI OPD sign convention?

1. The FITS files of the instrument do not obey an OPD sign convention, because only optical path lengths (between the instrument and the star) are provided, but no differences between these. The OPLs are encoded with the correct sign convention and an arbitrary offset (which means the common distance from a tangential plane that contains the projected baseline near the Earth to the star is discarded): Moving reflecting optical surfaces (the MDL mirrors, or the internal delay line mirrors) towards the star produces smaller numbers in the associated FITS binary table—consistent with [1, 3.5.3] which says that these columns ought contain the delays *applied*. (Here, *smaller* means *arithmetically smaller*, not smaller in absolute value.) Details are found in [18, 1.5.6], available in <http://www.strw.leidenuniv.nl/~mathar/public/VLT-TRE-MID-15824-0264.pdf>.
2. If, however, an application wants to apply the sign convention used in the ISS [31, 3.2.6.4], [18, 1.5.6] should be consulted to calculate a number which is consistent. According to this particular definition based on which beam is closer to some wall on Paranal, the contribution of the piezo motion plus the tracking commands sent to the MDL is

$$D = \text{OPD}[2] + \text{LOCALOPD}[2] - (\text{OPD}[1] + \text{LOCALOPD}[1] + \text{DLMT}), \quad (1)$$

where the (signed) value of the DLMT is found in the INS DLMT POS keyword in the primary header. This must be superimposed with the contribution by the blind tracking of the MDL to get a full picture of the total OPD (see Sec. IG). The value in Eq. (1) is positive if the combined action of the internal and main delay line made the OPL from the star shining through beam B to the detector longer (synonymous to: from the star shining through beam A shorter) than following from the ISS blind tracking model geometry alone.

The reason of this fixed association of FITS indices with this particular OPD sign convention is the simplicity of the feeding optics, see Sect. ID.

3. Astronomers should be aware that the OPDs *applied* carry some “intrinsic” sign which is opposite to the *external* OPDs of astronomical relevance, simply because the principal mode of operating delay lines keeps the total OPD close to the white light fringe such that the “total” OPD seen by the detector is close to zero: the OPD *applied* by one arm of the interferometer needs to be *smaller* if the OPL to the star is *larger*. In total, there are four different ways of defining this OPD (internal versus external plus an arbitrary choice of the “first” telescope) which results in two different sign conventions. Phase sign conventions add another ambiguity well known from Fourier transforms, which does not matter here.

C. Which of the two telescopes was closer to the star?

Some approaches to the answer are:

1. If one draws a line on the ground perpendicular to the baseline which cuts the baseline vector in half (an azimuth), this defines two opposite star directions along the line for which the answer is undecided, and defines two hemispheres of directions (of star azimuths) closer to the one or to the other telescope. Consider the position angles τ for the baseline directions as listed in <http://www.eso.org/observing/etc/doc/vlti/baseline/baselinedata.txt>, where τ is counted North through East seen from the first one. (All the links at the bottom of this ESO web page are broken (App. G1). One must add a subdirectory level `baseline` into these URLs to get links to information.) A bird's view for the case of a star declination that places it South is Fig. 1.

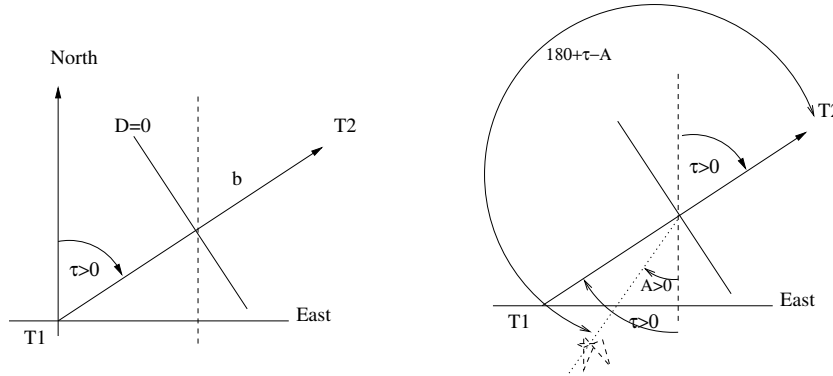


FIG. 1: In a topocentric coordinate system, the baseline direction is characterized by azimuth angles τ and $A_b \equiv \tau + 180^\circ$. In the case shown, $0 < A < \tau < 90^\circ$.

Further consider the azimuths A as taken from the ESO ISS AZ keyword in the primary header with the convention $A = 0$ for pointing to the south and $A = +90^\circ$ for pointing to the West (see <http://archive.eso.org/Tools/DidRep/DidRepWebQuery?did=ESO-VLT-DIC.ISS> and [39, §5.1.3]). This is the standard definition on the northern hemisphere, but not the one used in [40, 3.2.1] and [11]). T_1 sees T_2 under the azimuth angle $180^\circ + \tau$. A simple way to extract this number A is

```
dfits MIDI*.fits | egrep '(AZ|ARCFIELD)'
```

with the `eclipse` software, or

```
fitshead MIDI*.fits | egrep '(AZ|ARCFIELD)'
```

where available. A combined conclusion is: the star is closer to the first (left) telescope in the table if

$$|180^\circ + \tau - A| > 90^\circ, \quad (2)$$

else closer to the second telescope. The formula is valid for the normalizations $0 \leq A \leq 360^\circ$ and $-180^\circ \leq \tau \leq 180^\circ$. With a definition

$$A_b \equiv 180^\circ + \tau \quad (3)$$

for the baseline azimuth, it could also be written

$$|A_b - A| > 90^\circ, \quad 0 \leq A, A_b \leq 360^\circ. \quad (4)$$

2. The small numbers spread in the four `issgui` PostScript files of <http://www.strw.leidenuniv.nl/~mathar/vlti/> show the signed external delay in meters as a function of azimuth and elevation for all station pairs where the finite range of the delay lines may render some portion of the sky not reachable (in the sense of placing the ZOPD near a common point in the interferometric lab).

3. The Java applet shown on page 17 in <http://www.strw.leidenuniv.nl/~mathar/vlti/prErrWeb.html> has a well defined (but again arbitrary) sign convention as documented. It can be fed with the FITS keywords RA, DEC and LST of an existing primary header plus a pair of Paranal stations and emits a signed number. (Well, it does this in parallel for two stars and emits two numbers.) This number is larger than zero if the external path length from the star to what is called T1 in the applet is larger than the (external) path length to T2.
4. The interactive GUI by the Astrometric Preparation Software <http://obswww.unige.ch/~segransa/apes/> can probably be used as well.
5. One can compute the product of equations (13) and (14) as formulated in (15). The variable D used there is larger than zero and the angle θ smaller than 90° if the star is closer to T2.

The results of any of these approaches ought be consistent. All but one are redundant.

D. Which of the two telescopes collected beam A, which beam B?

By following the right angle turns of the 18 mm beams back we find:

1. Moving from the ARAL feeding optics [40, 4.5.4] [31, Fig 3.8.2-1] to the MIDI warm bench, beam A was the Western one.
2. Before hitting the ARAL feeding optics, beam A was the Northern one, beam B the Southern one.

Translation into the language of the “lab input beams” of [39, 3.2], the input beam number of beam A is larger than the input beam number of beam B, both ranging between 1 and 8 (once all DLs have been installed). By reverse lookup of the numbers of the two primary header keywords ESO ISS CONF INPUT1 and ESO ISS CONF INPUT2, one can get the information which of the two input beam numbers was coupled to the “first” and which to the “second” telescope. Then forward lookup with the keywords ESO ISS CONF STATION1 and ESO ISS CONF STATION2 gives the (station) names in the familiar nomenclature [40, Table 3-2]. Example:

```
HIERARCH ESO ISS CONF INPUT1 =    1      / Input channel in lab
HIERARCH ESO ISS CONF INPUT2 =    3      / Input channel in lab
HIERARCH ESO ISS CONF STATION1= 'U3     ' / Station of telescope 1
HIERARCH ESO ISS CONF STATION2= 'U1     ' / Station of telescope 2
```

Here $3 > 1$, therefore INPUT2 belongs to beam A. Therefore we have to follow the entry for STATION2 which tells us that U1 fed beam A.

E. Was the OPL of beam A longer than the OPL of beam B?

To the precision available from variables in the primary header, this question cannot be answered, since (see above) the *external* additional OPL to the telescope further away from the star is almost equally added to the other beam by the MDL while tracking the fringe. “Almost equally” means that dispersion effects in the air-filled delay lines, lensing by the Earth’s atmosphere etc [38] cause this to be true only for one “effective” point in the star spectrum.

If the question was in the sense of “Did beam A or beam B come from the telescope further away from the star?” the answer given by first answering the question in Section ID and moving with this answer on to Section IC.

F. Did the MDL passed by beam A or the one passed by beam B move?

As discussed in Section IA, LOCALOPD[1] or LOCALOPD[2] in equation (1) may change with time, LOCALOPD[1] always associated with beam A and LOCALOPD[2] always with beam B. The equivalent statement in *not* correct for OPD[1] and OPD[2], which means if for example OPD[1] does not change in time but OPD[2] does, nevertheless the MDL passed by beam A may be the one that moves, whereas the MDL passed by beam B may be standing (then baptized the “reference” DL). The MIDI software ensures that equation (1) remains correct, although the time-dependent numbers may have been swapped from OPD[1] to OPD[2] or the other way round, including a change in sign.

If the two telescopes are on different East-West sides of the tunnel, the two MDL are also on different sides [40, 3.2.3.2.4]; see [40, Fig 3-2] or [40, Fig 3-6] to figure out whether this is currently the case: UT1, UT2 and ATs on rails A–G are West-side, whereas UT3, UT4 and ATs on rails H–M are East-side. By looking at the keyword `DEL REF NAME` and with the enumeration of [40, Fig 3-6] one can quickly explore which of the two MDLs moved for this case. Example: if `DEL REF NAME = 'DL3'`, the MDL associated with one of the East-side stations was *not* moving, neither for blind tracking nor for the commanded offsets stored in the `OPD[]`.

However, if the current telescope pair was UT3+UT4 (both with larger U coordinates than the VLTI complex and both “East-side” telescopes), this information would still not tell whether DL3 was associated with UT3 or UT4 for a full answer, even though both delay line names are provided in `ESO ISS CONF DL1` and `ESO ISS CONF DL2`. In this case one may get the information needed from a model of the change of the external OPD with time; from there, the change of the OPL reported by `DEL DLT1 OPL END`, `DEL DLT1 OPL START`, `DEL DLT2 OPL END`, and `DEL DLT2 OPL START`—one pair constant the other one the relevant one— may be either showing an increase or decrease. This sign of the time derivative of the `DEL DLTi OPL` that moved encodes implicitly whether the MDL moved that was associated with the telescope closer to the star, or the one associated with the telescope further away from the star.

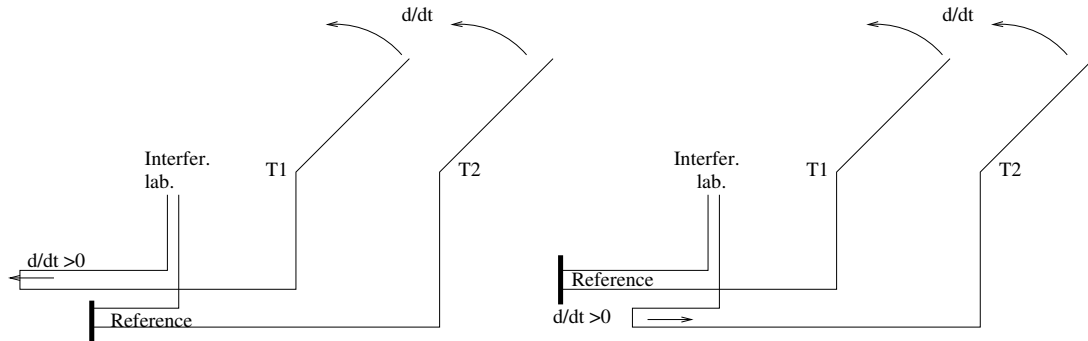


FIG. 2:

Fig. 2 shows two situations with a star moving closer to T_1 as a function of time, indicated by the curved arrows above the telescopes. On the left, the lower main delay line (the “reference”) does not move and the upper one needs to move to the left to “stay on the fringe.” On the right, the role of the active and reference delay lines was swapped, and the lower delay line must move to the right as a function of time. We may assume that both delay line positions refer to coordinate systems that provide a (positive) relative distance to the facing/opposite wall, which means that the sign of the time derivative of the MDL positions differs in the two cases.

The GUI `prErrWeb.html` shown on page 17 shows the external OPD in units of meter and also its time derivative in units of mm/s. In the graph above and with the sign convention used in the GUI, the OPD of the graph is positive and its time derivative negative; it is eventually the quotient of dD/dt by the time derivative off the moving MDL position (both of approximately the same absolute value) which matters: if close to -1 , the MDL of T_1 moves, if close to $+1$, the MDL of T_2 .

G. What was the actual external OPD?

The quickest way to compute the unsigned OPD $|D|$ is to use the vector equation

$$\mathbf{D} = \mathbf{b} - \mathbf{P} \quad (5)$$

in the form

$$D^2 = b^2 - P^2. \quad (6)$$

The baseline length b could be obtained

- according to $b^2 = (T1X - T2X)^2 + (T1Y - T2Y)^2 + (T1Z - T2Z)^2$ with values extracted from the primary header keywords `ESO ISS CONF T1X` etc or from the column `STAXYZ` in the table `ARRAY.GEOMETRY`.
- from the web page <http://www.eso.org/observing/etc/doc/vlti/baseline/baselinedata.txt>.

- via the geographic coordinates Φ (ESO ISS GEOLAT) and λ (ESO ISS GEOLON, including sign) of App. E 1, which are equivalent to the angle of separation Z between the two telescopes subtended at the center of the Earth, using [19]:

$$b = (\rho + H) \sqrt{2(1 - \cos Z)} = 2(\rho + H) \sin \frac{Z}{2} \approx (\rho + H) \left(Z - \frac{Z^3}{24} + \frac{Z^5}{1920} - \dots \right), \quad (7)$$

$$\cos Z = \sin \Phi_1 \sin \Phi_2 + \cos \Phi_1 \cos \Phi_2 \cos(\Delta\lambda). \quad (8)$$

A numerically stable evaluation would insert the Taylor expansion

$$2(1 - \cos Z) \approx (\Delta\Phi)^2 + \cos^2 \Phi_2 (\Delta\lambda)^2 - \frac{\sin(2\Phi_2)}{2} \Delta\Phi (\Delta\lambda)^2 - \frac{\cos^2(\Phi_2)}{2} (\Delta\Phi \Delta\lambda)^2 - \frac{1}{12} (\Delta\Phi)^4 - \frac{\cos^2 \Phi_2}{12} (\Delta\lambda)^4 \quad (9)$$

into the first equation, where $\Delta\lambda = \lambda_1 - \lambda_2$. The effective Earth sphere radius $\rho + H$ includes the mountain altitude ESO ISS GEOELEV. The major problem with this calculation is that the actual meaning of the GEOLAT keyword remains obscure: supposed it refers to a *geodetic* latitude, one would use the intermediate Cartesian coordinates [22] and the Pythagorean formula from the first bullet to calculate b .

The projected baseline length P at the start and end of the exposure is listed under ESO ISS PBL12 START and ESO ISS PBL12 END in the primary header.

H. How do piezo movements relocate the point of ZOPD on the sky?

1. Qualitative: Sign

Sky positions of equal OPD are concentric circles on the celestial sphere centered at the baseline vanishing point, see [38, §29]. On an imaging detector, they are lines. Which of the two baseline directions points to the circle's center depends on the sign of the OPD. Change of the internal OPD augments or shrinks the radius of this circle of ZOPD, as if one would select coherent light from a different position on the sky. This changes the star azimuth A (the point where this circle touches the observer's horizon), and with equation (4) one may say that this change moves the star closer to T_1 if $|A_b - A|$ increases, or else moves the star closer to T_2 if this absolute value decreases.

Normal interferometric VLTi operation tracks the star with the MDL such that the path length L_1 from the star through T_1 to the beam combiner equals the path length L_2 through T_2 to the beam combiner. Path lengths stretch over “external” plus “internal” parts,

$$L_1 = L_2, \quad L_1 = L_1^{\text{ext}} + L_1^{\text{int}}, \quad L_2 = L_2^{\text{ext}} + L_2^{\text{int}}. \quad (10)$$

Coherent with the rest of this script we adopt the sign convention

$$D \equiv L_1^{\text{ext}} - L_2^{\text{ext}} \quad (11)$$

for the external OPD. [There are four possible combinations of being closer to either telescope before the change and changing this closeness, equivalent to the “Kronecker product” of a sign in D and a sign in ΔD caused by a change in one of the L_i , and also equivalent to a sign of $|A_b - A| - 90^\circ$ and a change of this value.] The previous two equations yield

$$\Delta D = \Delta(L_1^{\text{ext}} - L_2^{\text{ext}}) = \Delta(L_1 - L_2 - L_1^{\text{int}} + L_2^{\text{int}}) = \underbrace{\Delta(L_1 - L_2)}_0 + \Delta(L_2^{\text{int}} - L_1^{\text{int}}). \quad (12)$$

If we define the MIDI piezo motion relative to its rest position, we have $\Delta L_i^{\text{int}} < 0$ since it pushes the roof top mirror towards the beam during the standard “ramp” as the voltage is applied and the piezo expands. If furthermore we have a motion driven by the standard templates, this moves the beam with index $i = A$, which is to be checked as described in Section IA. Furthermore $\Delta L_A^{\text{int}} < 0$ is equivalent to $\Delta L_B^{\text{int}} > 0$ with respect to ΔD , or equivalent to $\Delta L_B^{\text{ext}} < 0$, deduced from the equations above as the total path length is kept balanced between the two arms of the interferometer. In the nomenclature introduced above, this reduction in the external path length L_B^{ext} means the point on the sky moves towards the telescope of beam B: Figure 3.

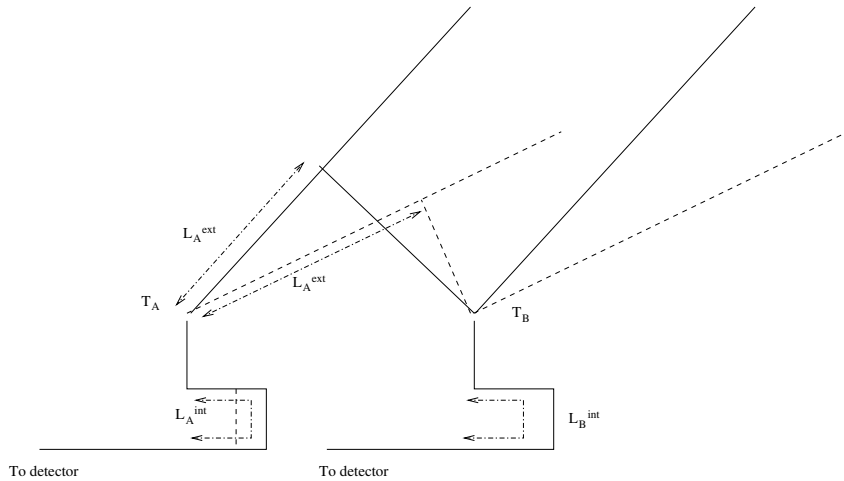


FIG. 3: If the internal path difference L_A^{int} for beam A is shortened by stepping the piezo such that it moves from the solid position to the dashed position, the effective pointing direction on the sky enlarges L_A^{ext} to “register” with a new direction of zero, coherent total OPD. This effectively chooses a pointing direction that moves closer towards the telescope of beam B.

2. Quantitative

We can work this out more quantitatively: We define the two geographic latitudes Φ_i and longitudes λ_i of T_1 and T_2 and from there the Cartesian coordinates of the baseline vector \mathbf{b}_{12} from T_1 to T_2 [17, 19]:

$$\mathbf{b}_{12} = (\rho + H) \cdot \begin{pmatrix} -\sin \Phi_1 \cos \Phi_2 \cos(\Delta\lambda) + \cos \Phi_1 \sin \Phi_2 \\ \cos \Phi_2 \sin(\Delta\lambda) \\ \cos \Phi_1 \cos \Phi_2 \cos(\Delta\lambda) + \sin \Phi_1 \sin \Phi_2 - 1 \end{pmatrix} \quad (13)$$

where $\Delta\lambda \equiv \lambda_1 - \lambda_2$, $|\mathbf{b}_{12}| = b$, where x points to the North, y to the West and z to the zenith at the location of T_1 , and where $\rho + H \approx 6380$ km is the effective Earth radius at the platform. Alternatively, one may generate the first two components of this vector by subtracting two of the e and n numbers from <http://www.eso.org/observing/etc/doc/vlti/baseline/vltistations.html> and setting the third to zero, or using the table in [32, §6.2.1].

The star direction is

$$\mathbf{s} = \begin{pmatrix} -\cos A \sin z \\ \sin A \sin z \\ \cos z \end{pmatrix} \quad (14)$$

in the same coordinates, with the Azimuth convention of Section IC. The external delay D is the dot product

$$D = \mathbf{s} \cdot \mathbf{b}_{12} = b \cos \theta; \quad 0 \leq \theta \leq \pi \quad (15)$$

with the sign convention that $D > 0$ and $\cos \theta > 0$ if the star is closer to T_2 than to T_1 . The cone angle θ of the circle of constant external OPD seen from the platform is

$$\cos \theta = \mathbf{s} \cdot \hat{\mathbf{b}}_{12}; \quad \hat{\mathbf{b}}_{12} \equiv \mathbf{b}_{12}/b; \quad P = b \sin \theta. \quad (16)$$

$\sin \theta$ is P , the value of the header keyword ESO ISS PBL12 START, divided by the value of b taken from [baseline-data.txt](#).

The (signed) change in OPD is related to the angular change $\Delta\theta$ of the ZOPD via the differential of (15)

$$\Delta D \approx -b \Delta\theta \sin \theta; \quad (17)$$

$$\Delta\theta \approx -\frac{\Delta D}{b \sin \theta} = -\frac{\Delta D}{P}, \quad (18)$$

where $b > 0$, $\sin \theta > 0$, $P > 0$. The recipe to calculate the signed $\Delta\theta$ is

- take P from the header as described in Section IG.
- Check as in Section IA whether the piezo of beam A or beam B moved, and obtain the local change ΔL (L is the total path length from the star to the detector. Up to some arbitrary constant, $-150 \mu\text{m} < L^{\text{int}} < 0$, but ΔL^{int} may have both signs depending on what one defines as the reference. If the reference is the rest position, $\Delta L^{\text{int}} < 0$.)
- (Note that the next step associates L with one of the telescopes and an “internal” delay, and that there are various equivalent ways of doing this as discussed above, only one of which is picked here.) Select one of the telescopes to be T_1 , the other T_2 , in accordance to the choice that defines the signs of Eq. (13) and (15). Figure out as in Sect. ID whether the piezo handled the beam through T_1 or the beam through T_2 . If the piezo modified the beam through T_1 , flip the sign of ΔL^{int} (as to relate L to the internal delay imposed by T_2).
- Define the ZOPD as given by (12),

$$\Delta D = \Delta L^{\text{int}} \quad (19)$$

and obtain the signed $\Delta\theta$ via (18).

The limitations for the piezo range ($|\Delta L| < 150 \times 10^{-6} \text{ m}$), the baseline ($b \geq 46.6 \text{ m}$ for UTs), and the zenith distance ($\theta \geq 30^\circ$) result in the limit $\Delta\theta \leq 6.4 \times 10^{-6} \text{ rad} = 1.3''$ obtained from (18). Larger ZOPD shifts must be relayed to the MDL.

The orthogonal projection of the change $\Delta\theta$ along the perimeter of the circle is only resolved through the PSF of the single telescope ($1.2\lambda/d = 0.31''$ for $d = 8 \text{ m}$ at $\lambda = 10 \mu\text{m}$, $1.2\lambda/d = 1.38''$ for $d = 1.8 \text{ m}$ at $\lambda = 10 \mu\text{m}$), the radial direction resolved proportional to λ/P of the interferometer. One may chose to associate $\Delta\theta$ not only with a change in the distance to the baseline’s line of sight, but also with a specific direction ($\Delta A, \Delta z$) in the tangential plane to the celestial sphere attached to A and z . Then from [38, §28.3.4]

$$(\Delta\theta)^2 = (\Delta z)^2 + \sin^2 z (\Delta A)^2 - \frac{1 + 2 \cos^2 z}{12} (\Delta z)^2 (\Delta A)^2 - \frac{1}{12} \cos^2 z \sin^2 z (\Delta A)^4 + \dots \quad (20)$$

The two components of the gradient are

$$\frac{\partial D}{\partial A} = \frac{\partial \mathbf{s}}{\partial A} \cdot \mathbf{b}_{12} = \begin{pmatrix} \sin A \sin z \\ \cos A \sin z \\ 0 \end{pmatrix} \cdot \mathbf{b}_{12}, \quad (21)$$

$$\frac{\partial D}{\partial z} = \frac{\partial \mathbf{s}}{\partial z} \cdot \mathbf{b}_{12} = \begin{pmatrix} -\cos A \cos z \\ \sin A \cos z \\ -\sin z \end{pmatrix} \cdot \mathbf{b}_{12} \quad (22)$$

by differentiation of (15). If one wants to calculate the direction $(\Delta A, \Delta z)$ of radial (steepest) change of the circle of ZOPD, for example, one would chose $\Delta A/\Delta z = (\partial D/\partial A)/(\partial D/\partial z)$, calculate the partial derivatives from the dot products in the previous two equations, divide (20) through $(\Delta z)^2$, and obtain Δz from (20). This approach works as well for the declination δ and right ascension α (or hour angle $h = \text{LST} - \alpha$, increasing with time, computed by subtracting the values of the FITS keywords LST and RA after scaling to common angular units) substituted for A and z in (14):

$$\mathbf{s} = \begin{pmatrix} \cos \Phi_1 \sin \delta - \sin \Phi_1 \cos \delta \cos h_1 \\ \cos \delta \sin h_1 \\ \sin \Phi_1 \sin \delta + \cos \Phi_1 \cos \delta \cos h_1 \end{pmatrix}; \quad h_1 - h_2 = \lambda_1 - \lambda_2. \quad (23)$$

A star at hour angle $h = 0$ is on the Meridian,

$$\mathbf{s} = \begin{pmatrix} \sin(\delta - \Phi) \\ 0 \\ \cos(\delta - \Phi) \end{pmatrix}, \quad (h = 0), \quad (24)$$

north of the zenith at $A = 180^\circ$ if $\delta - \Phi > 0$, south at $A = 0$ if $\delta - \Phi < 0$.

The dot product $\mathbf{s} \cdot \mathbf{b}_{12}$ between (23) and (13) is

$$D = (\rho + H)(\cos \delta \cos \Phi_2 \cos h_2 + \sin \delta \sin \Phi_2 - \sin \Phi_1 \sin \delta - \cos \Phi_1 \cos \delta \cos h_1). \quad (25)$$

$\Delta\Phi \equiv \Phi_1 - \Phi_2$ and $\Delta\lambda$ are small, measured in radian; from App. E1 we have $|\Delta\Phi| < 2.4 \times 10^{-5}$ rad and $|\Delta\lambda| < 3.1 \times 10^{-5}$ rad, the maximum North-South distance realized by the station pair B5–J6, and the maximum East-West distance by A1–M0. To avoid the massive cancellation of digits in (25), one would use the bivariate Taylor expansion

$$D/(\rho + H) \approx (\sin \Phi_2 \cos \delta \cos h_2 - \cos \Phi_2 \sin \delta) \Delta\Phi + \cos \delta \sin h_2 \cos \Phi_2 \Delta\lambda + \frac{1}{2} (\sin \delta \sin \Phi_2 + \cos \delta \cos h_2 \cos \Phi_2) (\Delta\Phi)^2 - \sin \Phi_2 \cos \delta \sin h_2 \Delta\lambda \Delta\Phi + \frac{1}{2} \cos \delta \cos h_2 \cos \Phi_2 (\Delta\lambda)^2 \quad (26)$$

The $\partial D/\partial\delta$ and $\partial D/\partial\alpha$ follow from there. For the details one must split the hour angle into a change in sky coordinate and a time difference $\Delta t = \Delta h + \Delta\alpha$, ie, judge to which degree the change in the piezo position has been instantaneous.

I. Phase measurements with MIDI

last change 6.5.2008, Ch. Leinert

The basic equations: Consider an object $P_\lambda(\alpha)$, where α is an angle on the sky. We write its one-dimensional Fourier transform i.e. its complex visibility, as $\mathcal{P}_\lambda(u) = \int_{-\infty}^{\infty} P_\lambda(\alpha) e^{-2\pi i u \alpha} d\alpha = |\mathcal{P}_\lambda(u)| \cdot e^{i\phi_\lambda(u)} = A_\lambda(u) \cdot e^{i\phi_\lambda(u)}$ with visibility amplitude $A_\lambda(u)$ and phase $\phi_\lambda(u)$. Reversing the direction in which α is increasing is equivalent to going from $P_\lambda(\alpha)$ to $P_\lambda(-\alpha)$ and would change the sign of $\phi_\lambda(u)$. Observing this object interferometrically with a baseline of projected length B_{proj} and a corresponding spatial frequency $u = B_{proj}/\lambda$ on the sky leads for multiaxial beam combination to a visualisation of the visibility component $\mathcal{P}_\lambda(u)$ as an instantaneous fringe pattern in the image plane with the modulating part

$$I_\lambda(x) \propto 2 |\mathcal{P}_\lambda(u)| \cos(2\pi f_m x + \phi_\lambda(u)), \quad (27)$$

where $1/f_m$ is the spatial fringe spacing and the sign of the phase is positive for proper choice of the sign of x . Alternatively, in coaxial beam combination this visibility component shows as an OPD-scanned timewise fringe pattern of

$$I_\lambda(\text{OPD}) \propto 2 |\mathcal{P}_\lambda| \sin(2\pi \text{OPD}/\lambda + \phi_\lambda), \quad (28)$$

where obviously $\Delta\text{OPD} = \lambda$ is the fringe spacing during an OPD scan. The latter method is used in the MIDI instrument on the VLTI. The presence of the sine function in relation (28) instead of the cosine function results from the well known $\pi/2$ phase shift in the symmetrically used beam splitter which brings about the coaxial recombination; the factor of two here results from taking the difference of the two beamsplitter output signals of opposite sign. As we will see, the $\pi/2$ phase shift is of no consequence for the phase determination of ϕ_λ . The positive directions of x in Equation (27) and OPD in Equation (28) need to correspond to the positive scan direction α over the source on the sky. Otherwise the phase ϕ_λ would change sign. In other words, defining the signs of x , resp. OPD and keeping Equations (27) resp. (28) also would define a positive direction α on the sky.

For later use we note that by the formulation of Equations (27) and (28), when ϕ_λ is going positive from the value 0 (which a point source at the origin would have), then the maximum, respectively the zero crossing of the fringe pattern (28) at the origin will move to negative values of x , respectively OPD.

Derivation from more general principles: Equations (27) and (28), though plausible, deserve some justification in detail, in particular to verify the sign of the angle α , of the OPD and of the phases. We start from Boden's presentation [2, p. 9]. A plane wave propagating from the object in direction \mathbf{k} towards the observer is written as $e^{i\mathbf{k}\cdot\mathbf{x} - i\omega t}$ with $|\mathbf{k}| = k = 2\pi/\lambda$. Using telescopes A and B we define the baseline vector \mathbf{B} as $A \rightarrow B$. Pointing the telescopes to the object, we are viewing in direction $\mathbf{s} = -\mathbf{k}$. The total optical path difference counted in the sense B minus A then is $\text{OPD} = -\mathbf{s} \cdot \mathbf{B} + d_B - d_A$, where d are the pathlengths from the telescopes to the locus of beam combination and $-\mathbf{s}\mathbf{B}$ constitutes the external part of the OPD which decreases for viewing directions towards telescope B. From the superposition of the waves travelling through telescopes A, $e^{i(\mathbf{s}\mathbf{B} + d_A) - i\omega t}$, and telescope B, $e^{i(d_B - i\omega t)}$, the fringe pattern results as

$$F_\lambda(\text{OPD}) \propto \cos(k(\mathbf{s} \cdot \mathbf{B} + d_A - d_B)). \quad (29)$$

To relate positions on the sky to the instrumentally available internal OPD $d_A - d_B$, we consider the viewing direction \mathbf{s} as origin on the sky. We take as zero point of OPD that value of $d_A - d_B$ where a point source at this origin would produce the white light fringe, i.e. where the argument of the cosine in Equation (29) is zero. We also note that with the accepted sign convention for the OPD (OPD = path length “MIDI beam B” minus path length “MIDI beam A”), an interferometric scan with MIDI moves the internal OPD $d_B - d_A$ stepwise towards more positive values, since the piezo motion is shortening d_A . In the actually used mechanical-geometrical setup, during such an OPD scan of the MIDI instrument the corresponding position of the white light fringe on the sky moves towards that one of the two used telescopes that sends its light beam into the right entrance window of the MIDI dewar, when seen with the incoming light (“MIDI beam B”). The fits headers of the stored data files carry the information which allows to transpose this somewhat convoluted definition into a defined direction on the sky such that the phases will give defined information on the object. It is natural to count α positive on the sky in the direction where the corresponding white light fringe moves during an internal OPD scan. According to Equation (29) this means that, because of d_A decreasing during the scan, α as $\mathbf{s} \cdot \mathbf{B}$ goes positive towards telescope B.

For an extended source we have to add the independent fringe patterns (Equ. 29) contributed from all its parts, which means integrating over α , which is in the plane of the sky and perpendicular to \mathbf{s} . The integrand then reads $P_\lambda(\alpha) \cdot \cos[k(\mathbf{s} + \alpha)\mathbf{B} - (d_B - d_A + \Delta\text{OPD}_{int})]$. Here, $d_B - d_A$ is the value of the internal OPD corresponding to the white light fringe at $\alpha = 0$, and ΔOPD_{int} is an intended instrumental offset from the white light position (describing, e.g. the piezo scan). Since $\mathbf{s} \cdot \mathbf{B} + d_A - d_B = 0$, the integrand simplifies to $P_\lambda(\alpha) \cdot \cos[k(\mathbf{s} \cdot \mathbf{B}) - \Delta\text{OPD}_{int}] = P_\lambda(\alpha)\cos(2\pi\alpha B_{proj}/\lambda)\cos(\Delta\text{OPD}_{int}) + P_\lambda(\alpha)\sin(2\pi\alpha B_{proj}/\lambda)\sin(\Delta\text{OPD}_{int})$. Keeping in mind the above definition of visibility $\mathcal{P}_\lambda(u)$, and respecting $k\mathbf{s} \cdot \mathbf{B} = 2\pi\alpha B_{proj}/\lambda$, the integral over α refers to the integrand $|\mathcal{P}_\lambda(u)|\cos(\phi_\lambda)\cos(\Delta\text{OPD}_{int}) - |\mathcal{P}_\lambda(u)|\sin(\phi_\lambda)\sin(\Delta\text{OPD}_{int})$ which directly leads to the form

$$F_\lambda(\Delta\text{OPD}_{int}) = |\mathcal{P}_\lambda(u)|\cos(2\pi\Delta\text{OPD}_{int}/\lambda + \phi_\lambda), \quad (30)$$

from which Equation (28) follows simply by applying the $\pi/2$ phase shift. This verifies the formulation of Equation (28), including the sign of the phase.

A Gedankenexperiment: We now consider a binary with the center of light in the origin to confirm by a detailed look at the expected temporal fringe pattern that the phases determined by MIDI will have the correct sign.

On the sky we are on safe grounds: The phase would show the form of a staircase with width of the individual steps in spatial frequency u of $\Delta u = 1/\text{separation}$ and the height of the steps depending on the brightness ratio. The phase will decrease with u if the companion is located at more negative α with respect to the primary. On the other hand, the binary’s phase with removed linear trend – as it is determined in the instrument MIDI – corresponds to a different position, namely with the primary at the origin. The binary phase now oscillates around zero. For a companion at more negative position α than the primary, the phase will increase with u (decrease with λ) at those spatial frequency values where the maxima of the visibility amplitude are found, a simple and useful criterion. *In the instrument* it looks like this: If we have a companion at slightly negative α with respect to the primary, its contribution to the temporal fringe would have a maximum slightly earlier in the OPD scan, at $\Delta\text{OPD}_{comp} = -\alpha \cdot B$. The maximum of the combined fringe pattern (primary plus companion) then will also be shifted to more negative values, by

$$\Delta\text{OPD}_{binary} = -\alpha \cdot B \cdot \frac{F_{comp}}{F_{prim} + F_{comp}}. \quad (31)$$

Measured in units of λ , this shift will decrease in absolute value, i.e. get more positive, rise with increasing λ . The phase ϕ_λ , corresponding to this shift of maximum, therefore will get more negative, decrease with λ . This has the correct sign, and so the phases determined from MIDI should be correct with the sign as defined by the Fourier transform and as used in equations (28) and (30).

The treatment of phases in MIDI: In MIDI, OPD in Equation (28) is the actual optical path difference for a given individual exposure. One such exposure with the MIDI instrument gives $F_\lambda(\text{OPD})$ as function of λ for the range 8–13 μm . Many of these exposures at a repeated sawtooth pattern of OPD steps scanning the fringe constitute an interferometric measurement. In each scan, the position of fringe maximum depends on the phase ϕ_λ .

For the determination of phases from MIDI measurements we have to recall that the total optical path difference consists of two parts of different behaviour: $\text{OPD}_{total} = \text{OPD}_{int} + \text{OPD}_a$, where the “instrumental” OPD_{int} is quickly stepped through a few times the wavelength of $\approx 10 \mu\text{m}$ during an interferometric measurement and is known including its sign, while OPD_a is mostly determined by the atmosphere and is more slowly varying with a few $\mu\text{m/s}$, but in an unpredictable way.

The EWS (expert workbench system) part of the [MIDI data reduction package](#) determines the phase by mathematically shifting each exposure as given by Equation (28) to OPD zero and then averaging to obtain the complex

visibility - modulus and phase [13][37, 3.2.4]. Remembering that a shift in image space (and here also in OPD) corresponds to a phase factor in Fourier space of the kind $e^{2\pi i u \text{OPD}}$, we multiply (28) by the factor $e^{-2\pi i u \text{OPD}_{int}}$ to “shift” each exposure $F_\lambda(\text{OPD})$ back to position $\text{OPD}_{int} = 0$. Equation (28) now reads - expressing the sine function by exponentials, and apart from factors which do not matter here -

$$F'_\lambda(\text{OPD}) = \frac{A_\lambda}{i} e^{2\pi i u \text{OPD}_a + i\phi_\lambda} - \frac{A_\lambda}{i} e^{-4\pi i u \text{OPD}_i - 2\pi i u \text{OPD}_a - i\phi_\lambda}. \quad (32)$$

To determine the unknown atmospheric optical path difference OPD_a , we Fourier transform (32) with respect to u and obtain peaks at $+\text{OPD}_a$ and $(-\text{OPD}_a - 2\text{OPD}_{int})$. Of these, the second term, rapidly changing with OPD_{int} during a scan quickly smears out by averaging over different exposures, so the only remaining peak gives the wanted value of OPD_a with correct sign. We now can perform the “shifting back” correction also for the atmospheric part of the OPD by multiplying equation (32) with $e^{-2\pi i u \text{OPD}_a}$. This leads to

$$F''_\lambda(\text{OPD} - \text{corrected}) = A_\lambda e^{+i(\phi_\lambda \pm \pi/2)}, \quad (33)$$

where we have omitted the strongly jittering part with the factor $e^{-4\pi i u \text{OPD}_i - 4\pi i u \text{OPD}_a - i\phi_\lambda}$. The constant $\pi/2$ results from the factor $1/i$, its sign depends on which of the two complementary interferometric signals after the beam splitter is subtracted from the other one. Averaging equation (33) over the typically several thousand exposures of an interferometric measurement thus will reliably determine —apart from a constant known in principle— the wanted phase $\phi_\lambda(u = B_{proj}/\lambda)$ over the wavelength range 8–13 μm . (At the same time, it will also give the visibility amplitude A_λ). We remove any linear trend with u from this phase, since it simply would correspond to a position offset of the source from the origin. As well we remove any remaining constant term $\neq 0$. Again apart from our constant, this term could be and appears to be mostly due to differential longitudinal dispersion over the unequally long air paths of the interfering light beams and it thus mostly carries information not related to the object. Of course, subtraction of the constant term also takes care of the added $\pm \pi/2$. This ends the determination of phase. We note that the data reduction procedure described here preserves the sign of phase as defined by the Fourier transform and given in Equation (28).

The phases determined with MIDI on the VLTI thus are not fully complete, with the constant and linear terms set to zero. But they allow e.g. to break the ambiguity of where the companion in a binary is located with respect to its primary. This property of the MIDI data is needed and used in the discussion of the close binary T Tau S above.

A check by a known binary: We wanted to check the signs of phase derived above from “first principles” with an object where we assume we know the position of the companion. The close binary Z CMa, with separation of $0.1''$, consists of an infrared companion and an FU Ori component. At 4 μm the infrared companion is brighter by a factor of 6, this ratio rising with wavelength. The ratio of correlated fluxes at 10 μm , determined is in the range 5–10. We conclude that with these clear inequalities the component much brighter at 4 μm will also be the much brighter component at 10 μm and that it also will show the larger correlated flux. We reject alternative numerically possible explanations like a no longer rising flux ratio for $\lambda > 4 \mu\text{m}$ with a visibility of the infrared companion at 10 μm 30–60 times smaller than that of the FU Ori component. Z CMa then can be used for calibrating the sign of the phase relation, and we did so with the result that the relations derived in this appendix appear correct.

II. IMAGING INFORMATION ENCODED IN MIDI FITS FILES

A. Where is North in the VLTI beams?

1. Without DDL or STS

The calculation of the field rotation angles ϕ in the beams that propagate into the Western direction in the VLTI laboratory according to formulas found in [11] or [31, §3.2.5.1] can be done with the shell script `mioFieldAng` which is available from <http://www.strw.leidenuniv.nl/~mathar/progs/mioFieldAng>. For the case of UTs used—as usual—with beam compressor, this results in

$$\phi = p - a - A + 167.02^\circ \quad (34)$$

where p is the parallactic angle [21] A the azimuth as given in the MIDI FITS header, and a the elevation of the object. (This equation is adapted from [31, (Tab 3-3)]; the sign of A is flipped to transform the azimuth conventions [10].) `mioFieldAng` computes ϕ for the ATs as well. Note that the results may be incorrect if

- The ATs field rotator angle is non-zero,
- ATs are equipped with the star separator (year 2008 or perhaps later),
- beams are passing by the PRIMA differential delay lines (year 2008 or perhaps later)

2. *With DDL and/or STS*

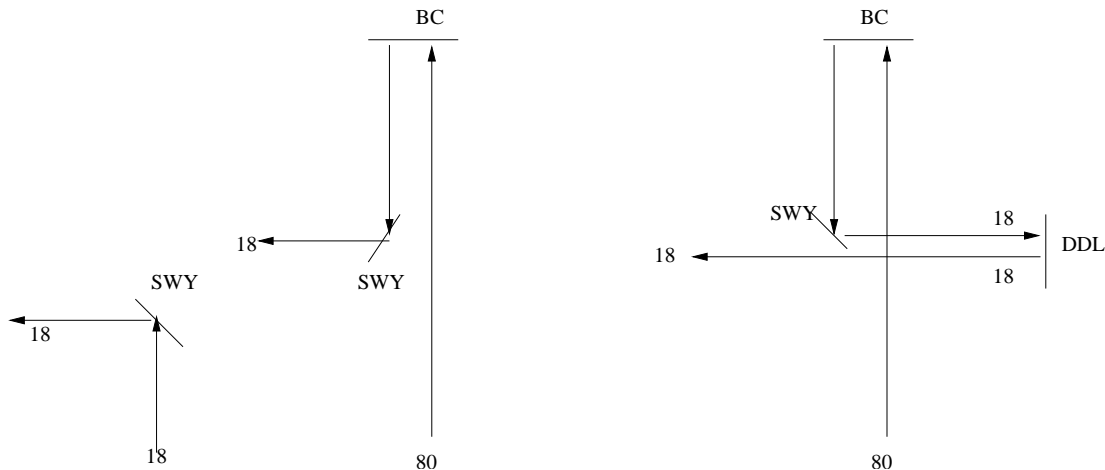


FIG. 4: Change of the beam path in the VLTI laboratory [26] when switching from the AT SF (left) or the AT DF or UT (middle) to the AT/UT DF mode (right). Numbers are beam diameters in mm. The rightmost case is probably irrelevant since the windows of the “vacuum” option of the DDLs have not been designed for N-band transmission [20].

Introducing the DDL into the beam changes the paths from one of the two layouts at the left of Fig. 4 to the one at the right. All three cases include one flat mirror of the SWY which therefore yields no net difference with respect to field rotation. The BC or the DDL (Figs. 9, 10) each have the same individual effect on the field rotation: building a mirror inversion upside-down (always looking into the direction of beam propagation); cascading both as in the right part of Fig. 4 eliminates their net effect. In total, the effect of incorporating the DDL adds to [11] the following rotations/inversions in the laboratory:

- an additional inversion upside-down for UTs, which flips the sign of ϕ (since this has been defined relative to a horizontal coordinate) and changes the formula $\phi - 90^\circ$ for the East angle to $\phi + 90^\circ$ [31, Tab. 3-3],
- no effect for ATs compared to the case without STS and without DDL.

(We neglect the case of using the ATs with STS, with BC but without DDL.) In addition, there is predictable contribution within the STS relative to the case of a straight two-mirror layout. Since I have no immediate information on the optics of the STS of the UTs (this is one mirror less than the STS of the ATs), only the case of adding the STS to the AT is summarized here. We replace the three-mirror arrangement M9–M10–M11 of the AT SF layout as shown in Fig. 8 by the layout of derotator and STS shown in Fig. 30 in [38] and Fig. 5 here.

- For the derotator in its nominal position, the image rotation of both cases of the AT Coudé train is the same.

Summarizing with the description of the effect in the VLTI lab, adding derotator in its nominal position, STS, BC and DDL have the same beam rotation effect for ATs as leaving all these components out. For general positions of the derotator, one needs to add (or subtract, pending a sign definition of the corresponding angle which—one would hope—will be made by ESO at some time in the future corresponding to the position angles) its field rotation angle (which is twice the angle of the mechanical rotation around the vertical axis).

This information is presumably correct for all VLTI instruments with the exception of anything parked on the Visitor’s Instrument Table (for example GENIE).

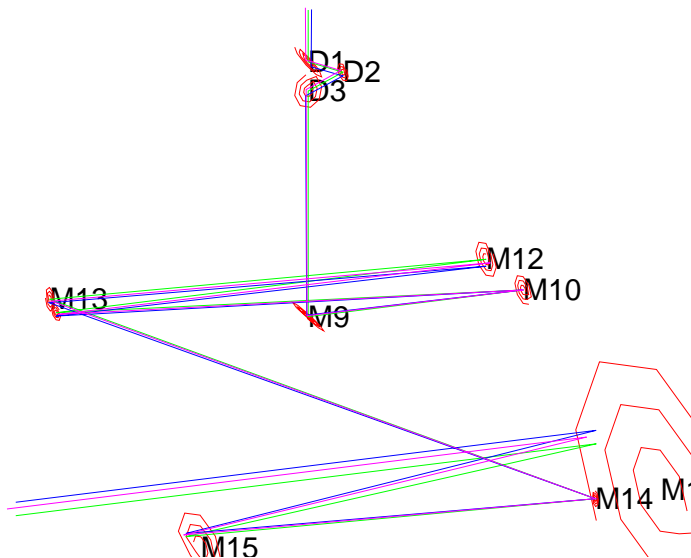


FIG. 5: Tracing the effect of the derotator and STS on the beam rotation.

B. Where is North on the MIDI detector?

The result of an image tracing of the coordinates mentioned in the previous section through the MIDI feeding mirrors and cold optics looks as in Fig. 6 [14] (images are not to scale).

In the two graphs above for the photometric channel of beam B, the green line approaches the MIDI feeding optics on the optical axis, the blue line is shifted a little into the $+V$ direction (displaced to the North) and the purple line is shifted a little into the $+W$ direction (displaced to the ceiling). These are reflected by the feeding optics and pass by the internal delay line of the warm optics, here labeled W1 to W4, with no net rotational effect. (W2 and W3 are driven by a single piezo, the equivalent optics of the other beam is not shown and driven by the other piezo.) They move on to M1 to M3 in the cold optics with the intermediate focus between M1 and M2. The second graph shows one arm of the photometric beams coupled out with the mirror named P, reflected by M4 and M5, and approaching the camera CAM, equivalent to the P_B channel in [12, Fig. 10]. Removing P and M4 as to represent the interferometric channels would have no net rotational effect, as comparison of the footprints of the beams that leave M3 and of the beams that leave M4 shows. After the switchyard, before the feeding optics, the blue ray was to the right and the purple ray above the green one—always as seen into the direction of light propagation. Before the camera, the blue line is below and the purple ray to the left of the green one. The camera lens inverts this when it creates the image, which leads to summary in Fig. 7 for both interferometric beams I_1 , I_2 , and both photometric beams P_A and P_B :

In the left diagram, we show the field angle ϕ in a coordinate system as if one was looking from the switchyard to the instruments and feeding optics in the VLTI lab, into the $-U$ direction, as defined in [11]. Note

- this diagram shows an image of the sky directions as if one had inserted a virtual single lens at some U coordinate which created the image on a sheet of paper in the (V, W) plane [9].
- The angle is *not* the same as values for the ROTATION column of the IMAGING_DATA tables defined in [1]. A C++ program `mioFitsPost` is available from the author's web page <http://www.strw.leidenuniv.nl/~mathar/progs/> which fills the ROTATION column with the time-dependent angles $\phi + 180^\circ$ for UTs and $180^\circ - \phi$ for ATs, wrapped into the interval 0–360°.

This ϕ would be obtained from the procedure of Section II A. On the right, the equivalent angle is shown on the MIDI infrared detector from the point of view of the incoming light, looking towards the detector with the beam combiner behind the back. The summary is that the detector watched from the front side (not from the mounting side) or one of the FITS images in the DATAi columns of the IMAGING_DATA table shows a true image for UTs as one would display a field on the sky, although rotated. The Java applet of the <http://www.strw.leidenuniv.nl/~mathar/vlti/prErrWeb.html> shown on page 17 also provides this information in the circular gridded area, where North and East are in the directions marked N and E.

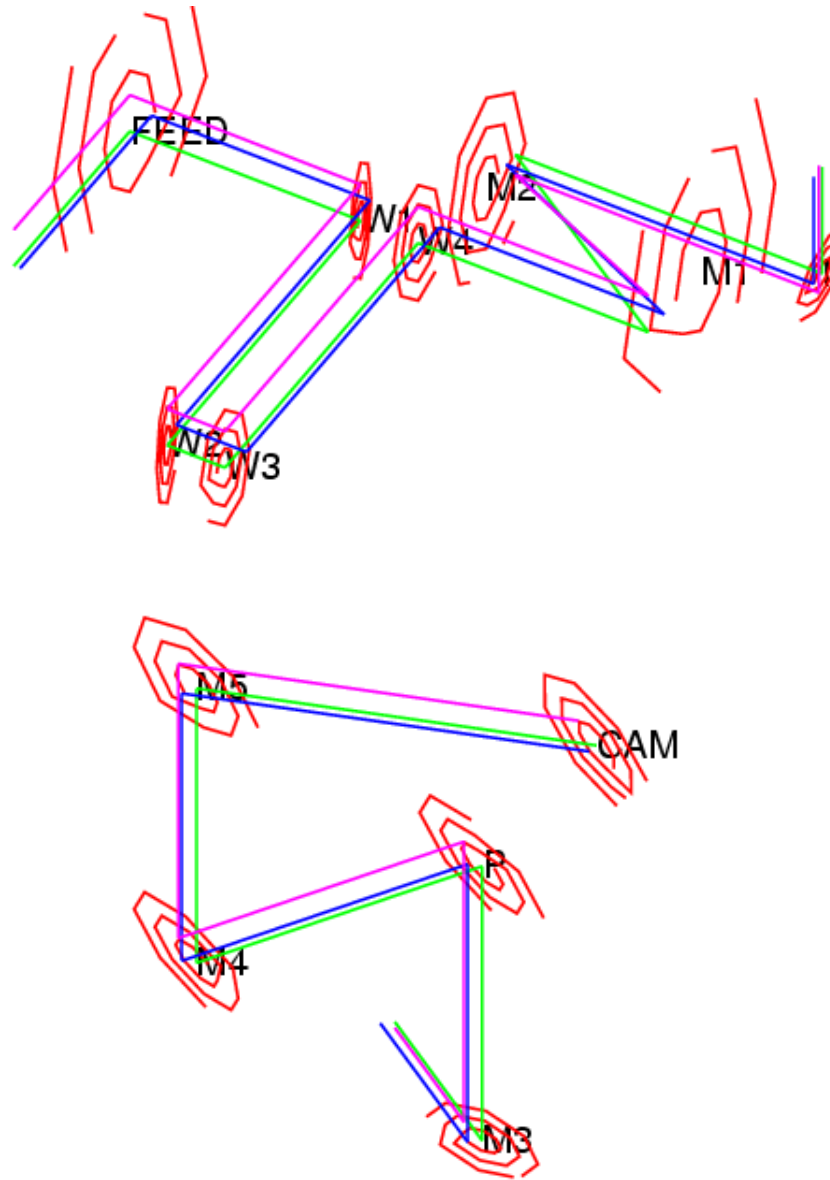


FIG. 6: Evaluation of the field rotation across the MIDI feeding optics, the warm optical bench up to the camera lens.

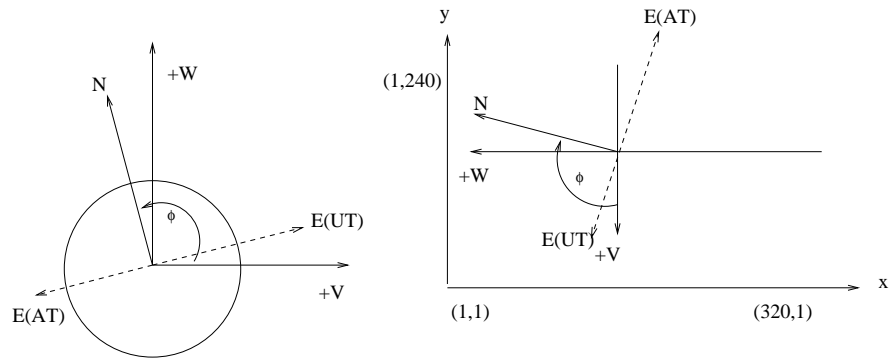


FIG. 7: At the left, the image rotation angle ϕ in the VLT tunnel coordinates (V, W) . At the right, the same field after transmission through the feeding optics, MIDI warm and cold bench and MIDI camera, in the 320×240 pixels in (x, y) FITS coordinates.

File Edit View Go Bookmarks Tools Window Help

Back Forward Reload Stop <http://www.strw.leidenuniv.nl/~mathar/vlti/prErrWeb.html>

Home Fedora Project Portal Latest Release Not... Fedora Community Red Hat Magazine

U1 long. (deg) -70.40507598184645 +- 0E0 lat. (deg) -24.627622066658432 +- 0E0 altit. (m) 2681.0 +- 0E0

Geoid: WGS84 inverse flatten.: 298.257223563 equatorial radius (m): 6378137.0

T1: U1
T2: U2

PS: RA: 02:42:40.81 Err RA (as): 0.3 DEC: -00:00:48.5 Err DEC (as): 0.3
SS: RA: 02:42:40.83 Err RA (as): 0.3 DEC: -00:00:48.4 Err DEC (as): 0.3

LST T1 (sec): 20729.25272876383 +- 1.4E-5

Update below!

star separation (arcsec) 0.3162277581537909 +- 7.6E-1 star orientation (deg) 71.56505071108042 +- 1.4E2

T1 XYZ Geocen (m): 1946396.6677840326 +- 0E0 -5467649.648108634 +- 0E0 -2642751.601785506 +- 0E0
T2 XYZ Geocen (m): 1946427.1358481874 +- 0E0 -5467661.185236289 +- 0E0 -2642705.601792468 +- 0E0

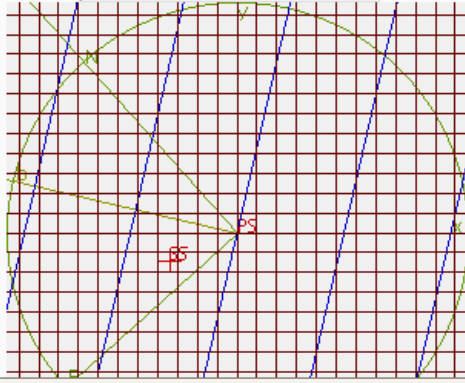
baseline (m) 9.580501969915517 +- 0E0 proj. basel. orient. angle (deg) 35.10963963733059 +- 6.1E-6

PS T1: A (deg): 67.88640689919019 +- 1.5E-4 z (deg): 50.58289464526917 +- 1.2E-4 p (deg): 122.63043281477748 +- 9.5E-5
PS T2: A (deg): 67.88692573393195 +- 1.5E-4 z (deg): 50.582929218465836 +- 1.2E-4 p (deg): 122.62977660248518 +- 9.5E-5
SS T1: A (deg): 67.88631845322422 +- 1.5E-4 z (deg): 50.582839443078306 +- 1.2E-4 p (deg): 122.63048895499101 +- 9.5E-5
SS T2: A (deg): 67.88683728882822 +- 1.5E-4 z (deg): 50.582874015492415 +- 1.2E-4 p (deg): 122.62983274210997 +- 9.5E-5

OPD PS (m): -2.9744542493460746 +- 1.1E-4 OPD SS (m): -2.9743845670568976 +- 1.1E-4
DOPD (mm): -0.06968228917703101 +- 2.3E-1
OPD PS (mm/s): -2.3635282234214454 +- 3.1E-7 OPD SS (mm/s): -2.3635285371462382 +- 3.1E-7
DOPD (um/s): 3.137247928108877E-4 +- 6.3E-4

MIDI 2"
um/line 20
FIELD pix Grid

zoom 1



Applet prErrWeb started

C. How does the baseline project onto the sky?

The projection of the baseline onto the celestial sphere is summarized in [21, 23] and section IIA of [24]. The azimuths A_{Tel1} and A_{Tel2} of the telescopes that define the baseline can be obtained from the file `baselinedata.txt` where for each allowed telescope pair one finds the baseline length b , and a quantity called `Pos.Angle` τ , which actually is an azimuth counted north over east. Seen from the mid-point of the baseline, telescope 1 then is at azimuth τ , telescope 2 at azimuth $A_b = \tau + 180^\circ$, see Fig. 1 above. The object's azimuth A are from the hierarchical keyword `ESO ISS AZ` and the object's elevation a from `ESO ISS ALT`, both referring to the start of measurement. Note:

- The Paranal zenith direction is currently not better defined to better than $530''$ or 0.14° (see App. E2). The use of a horizontal system with the variable a implicitly defines the correct tangential plane for the purposes of this script here. If the Paranal W coordinate between the two telescopes differs—see the `STAXYZ` column in the `ARRAY_GEOMETRY` binary table—an intermediate transform from this Cartesian UVW coordinate system to the horizontal system used here might be necessary.

The parallactic angle p is available in the primary header keyword `ESO ISS PARANG`.

OIFITS [28, 29, 41] defines an x -axis pointing to the East and a y -axis pointing to the North, but no associated angle. Our convention implies $x \propto \sin p_b$ and $y \propto \cos p_b$ which is different from the Calabretta-Greisen azimuth convention, Fig. 3 and formulas (12)–(13) in [3], who start at an angle of zero along the negative y -axis.

Quick interactive ways to obtain p_b are

- to start the Java applet <http://www.strw.leidenuniv.nl/~mathar/vlti/prErrWeb.html> shown on page IIB, select the two stations, insert the star coordinates at PS: RA and PS: DEC, the sidereal time labeled LST, click on `Update below!` and read the value of `proj. basel. orient. angle`.
- or to start the Java applet <http://obswww.unige.ch/~segransa/apes/>, select baselines and star coordinates, and read off the value of `Theta`.
- The values of A_b and p_b are also reported by recent versions of <http://www.strw.leidenuniv.nl/~mathar/progs/mioFieldAng>, which scans the FITS files of an entire UNIX directory.

The resulting position angle for the projected baseline may be compared with the output of the routine `baseline.pro` under MIA+EWS (which may have been calculated for a different time than the start of the measurement, however). The angles p_b or ψ are not given in the primary header of the MIDI data `*.fits` files prior to July 2006.

Programmers would probably use the `SLA_DBEAR` function of the `SLALIB`. Remarks:

- Since approximately June 2005, ISS adds two keywords `ESO ISS PBLA12 START` and `END` to the primary FITS headers, which are *not* directly related to θ or p_b . These header keywords are derived from the projected baseline vector \mathbf{P} . If \mathbf{P} is projected onto the (U, V) plane of the Paranal platform, the azimuth angle of this horizontal, doubly projected vector angle is reported in `ESO ISS PBLA12`, modulo 180° . At small delay D , the direction of \mathbf{P} becomes parallel to \mathbf{b} and the value of this keyword approaches τ or $\tau \pm 180^\circ$. The major difference between this implementation and the one formulated above is that the formulation of this script here is compatible with the OIFITS standard [28, App A] which explicitly defines the plane for the visibility calculation to be normal to the direction of the phase center. A change request has been issued as `SPR VLTSW20060066`, see App. E4. Inspection of MIDI data files of Sep. 2006 shows that the values of `ISS PBLAij` are still the Gitton angles A_G that one might define by decomposing the projected baseline vector \mathbf{P} in the topocentric coordinate system, North over East. Subsequent inspection of MIDI data files obtained with the ATs in April 2007 suggests that the values of `ISS PBLAij` then agree with p_b .
- The diurnal motion of the angle p_b is the same as known from the conventional (U, V) tracking plots, since moving between Fourier-conjugated variables preserves angles (and generally the dependence on spherical harmonics).

The time dependence of p_b is known from the $u - v$ plots and more complicated than the sinusoidal motion of the delay D . Illustrative plots of p , p_b and ψ as a function of time are shown in [20] which is available from <http://www.strw.LeidenUniv.nl/~mathar/public/UL-ICD-DDL-15728-0009.pdf>.

Appendix A: Baseline Azimuth Angles

The baseline orientation τ from T_1 to T_2 in the notation of <http://www.eso.org/observing/etc/doc/vlti/baseline/baselinedata.txt> is zero if T_2 is north of T_1 , and $+90^\circ$ if it is East of T_1 : Fig. 1. (Note that the tables

in [7] use a different definition.) In the limit of zero eccentricity of the Earth ellipsoid, the angle can be computed by plugging [22, (A19)] into [22, (78)],

$$c_3 \equiv (\rho + H) \frac{\cos \Phi_1 \cos \Phi_2 \sin(\lambda_2 - \lambda_1)}{\sin Z}; \quad (\text{A1})$$

$$\tan \tau = \frac{c_3}{\sqrt{(\rho + H)^2 \cos^2 \Phi_1 - c_3^2}}, \quad (\text{A2})$$

where Z is defined with (8), and where

$$\mathbf{T}_i \equiv (\rho + H) \begin{pmatrix} \cos \lambda_i \cos \Phi_i \\ \sin \lambda_i \cos \Phi_i \\ \sin \Phi_i \end{pmatrix} \quad (\text{A3})$$

are the Cartesian telescope coordinates in the geocentric rest frame, compatible with OIFITS [28, 29]. For higher accuracy with non-zero eccentricity, my program <http://www.strw.leidenuniv.nl/~mathar/progs/Geod.java> can be compiled and run.

Note that, strictly speaking, τ does not transform into $\tau \pm 180^\circ$ if the roles of \mathbf{T}_1 and \mathbf{T}_2 are swapped, because the great circles that fixate the τ in the two tangent planes at either telescope are not *loxodromes*.

The transition from the position coordinates of the `ARRAY_GEOMETRY` table defined in [1]—apparently a left-handed Cartesian coordinate system with the Y axis along the Greenwich meridian—to the `OI_ARRAY` table of [28, 29]—a right-handed coordinate system with the X axis along the Greenwich meridian—works as follows: The OIFITS header value `ARRAYX` is set to the VLTI header value `ARRAYY`. The OIFITS header value `ARRAYY` is set to the VLTI header value `ARRAYX`. The OIFITS header value `ARRAYZ` is copied over from the same VLTI header value `ARRAYZ`. The OIFITS values in the tabular column `STAXYZ` are constructed from the VLTI values in the tabular column `STAXYZ` by transformation of the VLTI local Alt-Az system to the OIFITS coordinate system which is (again) geocentric. The VLTI table values `STAXYZ[1,2,3]` are the coordinates $v_{1,2,3}$ in a system with the first coordinate to the West, the second to the South and the third to the zenith, or in terms of the unit vectors defined earlier in this section, the vector $-v_1 \hat{\mathbf{E}} - v_2 \hat{\mathbf{N}} + v_3/(\rho + H) \hat{\mathbf{T}}$. (The 19° -rotation from the Paranal (U, V) to a compass system has already been done within the ISS.) We assume that the origin in this coordinate system, $v_1 = v_2 = v_3 = 0$, equals the tail of the vector described by `ARRAY[XYZ]`. Let us call the three values in the OIFITS `STAXYZ` $o_{1,2,3}$; they are found by equalizing both representations in the same geocentric (earth-fixed) coordinate system:

$$-v_1 \hat{\mathbf{E}} - v_2 \hat{\mathbf{N}} + v_3/(\rho + H) \hat{\mathbf{T}} = o_1 \begin{pmatrix} 1 \\ 0 \\ 0 \end{pmatrix} + o_2 \begin{pmatrix} 0 \\ 1 \\ 0 \end{pmatrix} + o_3 \begin{pmatrix} 0 \\ 0 \\ 1 \end{pmatrix}. \quad (\text{A4})$$

This is solved by

$$o_1 = v_1 \sin \lambda + v_2 \cos \lambda \sin \Phi + v_3 \cos \lambda \cos \Phi; \quad (\text{A5})$$

$$o_2 = -v_1 \cos \lambda + v_2 \sin \lambda \sin \Phi + v_3 \sin \lambda \cos \Phi; \quad (\text{A6})$$

$$o_3 = -v_2 \cos \Phi + v_3 \sin \Phi, \quad (\text{A7})$$

where the coefficients form an orthogonal rotation matrix. The value of λ is the negative of the primary header's `ESO_ISS_GEOLON` multiplied by $\pi/180$, and the value of Φ the value of the `ESO_ISS_GEOLAT` multiplied by $\pi/180$. The numbers ought be compatible with those shown in the two lines with `Geocen` numbers in the GUI of page [II B](#).

This calculation is inaccurate if the representation with the VLTI keywords Φ and v_i is of mixed type (Φ in geodetic and v_i in geocentric coordinates or the other way round), on which I have no information (see App. [E 2](#)). If this mixed representation occurs, correction of Φ into the same system as v_i according to the standard formulas [34, §9][35] is needed as a preparatory step before the rotation matrix can be applied. The basic maths of this is summarized in App. [F](#).

Appendix B: Head files of split exposures

Some hints on figuring out which of the files in a directory might be such “head” files of an exposure:

- Exposures are scheduled by the instrument software to start on straight seconds (w/o chopping) or on times commensurable with the chopping period. Since the chopping frequency is often 2 Hz, files with “straight” millisecond identifiers like `MIDI*.000.fits` and `MIDI*.250.fits` are usually the first ones of an exposure, whereas those with some random milliseconds like `MIDI*.376.fits` are the followup files.
- If the keyword value of `ORIGFILE` in the FITS header ends on `_01.fits`, it is such a head file, whereas a higher index like `_02.fits` of the keyword value characterizes followup files.
- If the keyword value of `ESO_OCS_EXPO_FILENO` in the FITS header is 1, it is such a head file. The other files show higher integers 2, 3... with this keyword.

For UNIX directories with the raw MIDI FITS files, the head files can simply be listed by

```
ls -l MIDI.????-??-??T?:?:?:?.???_01.fits
```

For directories assembled by the ESO pipeline, one might use

```
fitshead MIDI*.fits | egrep '(ORIGFILE|ARCFILE)' | \
awk '{if (NR%2 ==1) n=strtonum(); else if (n==1) print $3}'
```

to list them. A C program `mioFitsFNames.c` that re-links a directory with files named according to the original instrument convention into another directory with the pipeline naming convention is available on the `mididata` account on the MPIA server `sun47`.

Appendix C: Pupil rotation in the VLTI train

In a color encoding consistent with the one above, the transversal of the beam for a UT pointing to the zenith looks as follows in the overview:

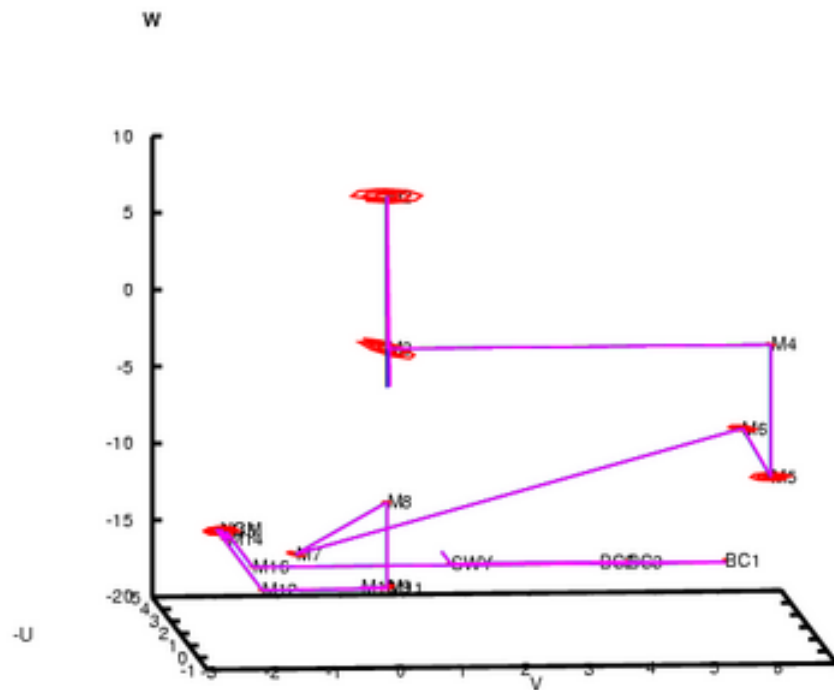


FIG. 8: Overview of the VLTI mirror train.

The uppermost mirror is M2, the one below M3; M1 is not shown. A detail of the three mirrors of the beam compressor looks as follows:

One more horizontal turn by the SWY mirror moves the beam leaving BC3 onto the feeding optics shown in Section II A. Zooming into the M13–M15 of the MDL it looks as follows:

Because the positions of the mirrors of the UT Coudé train are unavailable to the author, and a model of the foci higher up could not be made, we do not follow the rays further back through the optics.

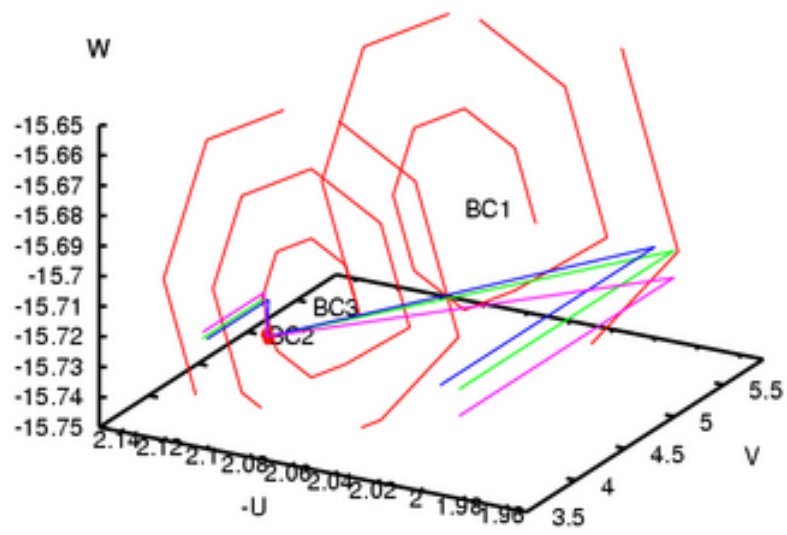


FIG. 9: Field rotation by the three reflections within a beam compressor.

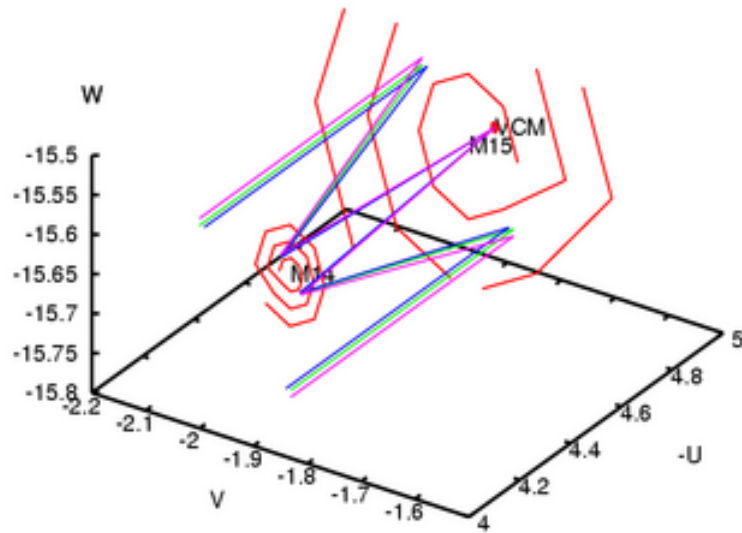


FIG. 10: Field rotation by the five reflections within a cat's eye of the MDL or DDL.

Appendix D: Atmospheric N band transmission

A detailed transmission spectrum of the Earth atmosphere is reproduced in Fig. 11. The N band is limited at short wavelengths by H_2O and CH_4 absorption, at longer wavelengths by CO_2 absorption [4, Fig. 11.6]. Correlated line list

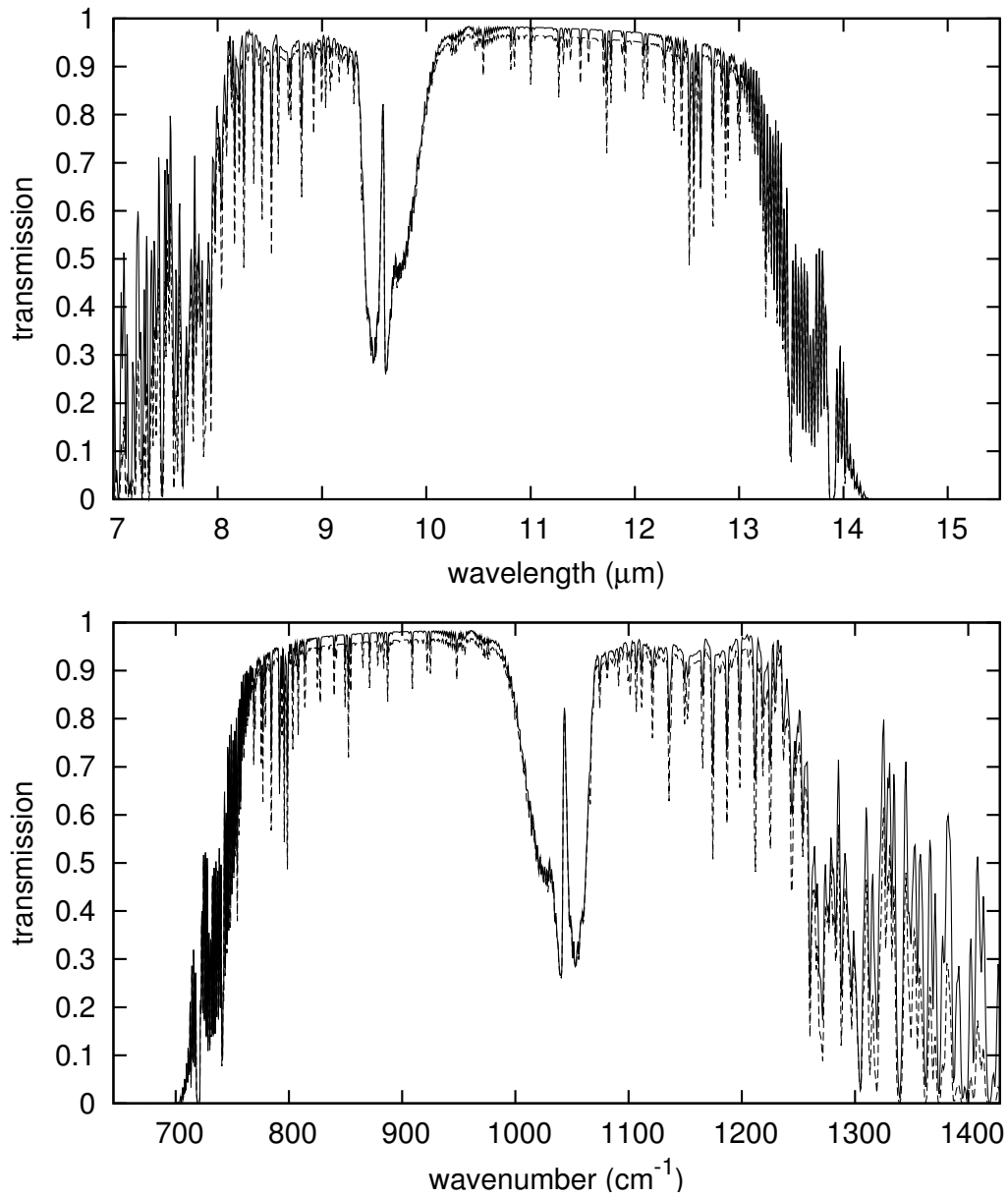


FIG. 11: Synthetic Mauna Kea sky transmission in the N band at an airmass of 1.5 and a 1 mm water vapor column (solid line) or 3 mm vapor column (dashed line) [15]. Sky transmissions in the IR bands have also been plotted in a work related to VLT/ISAAC [8], in the ISAAC User Manual [16, §3.1], and for VINCI [5].

representation of transitions found in the HITRAN database [33] is given in Figs. 12–13.

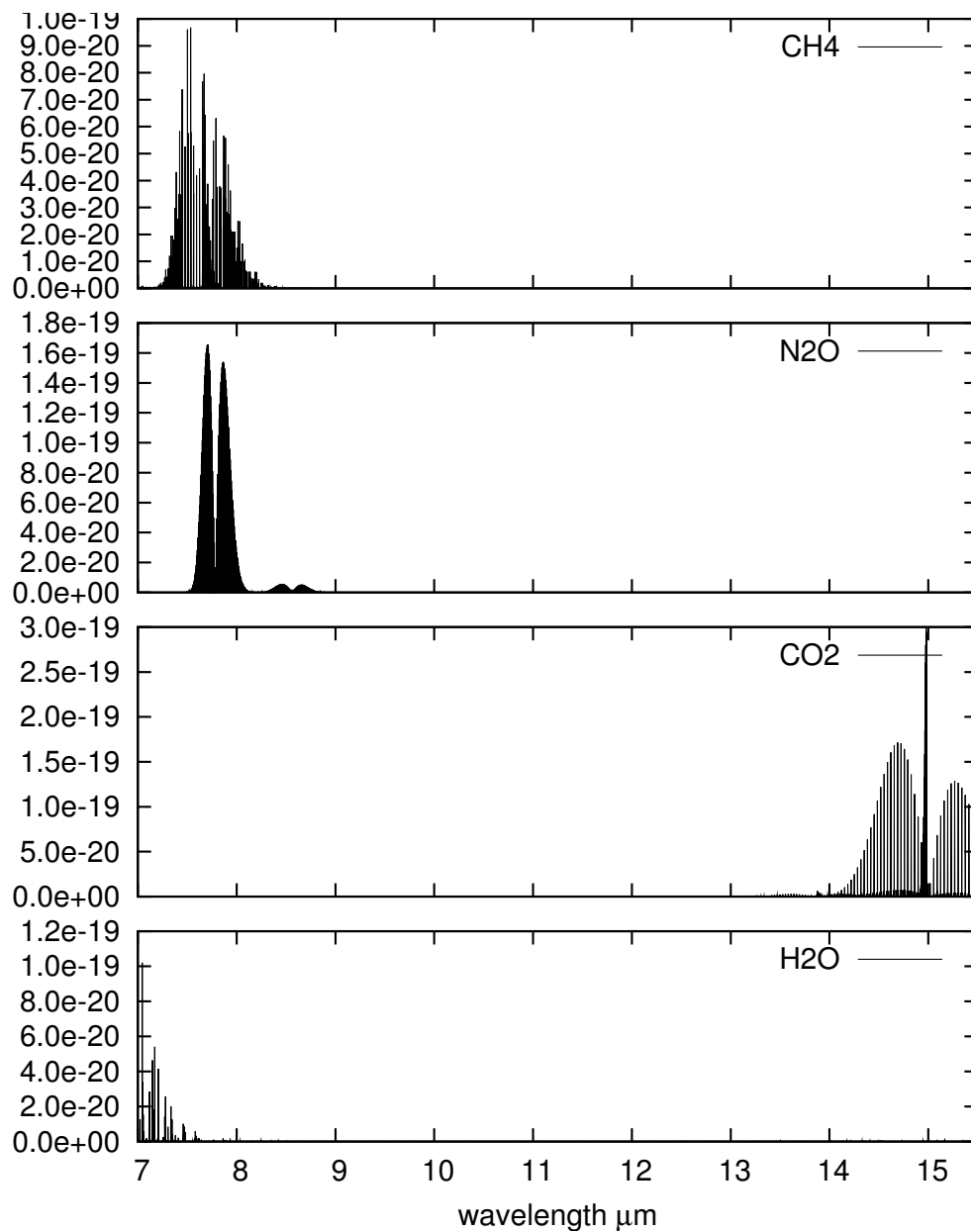


FIG. 12: HITRAN line locations and line strengths in units of $\text{cm}^{-1}/\text{molecule cm}^{-2}$ for CH₄, N₂O, CO₂ and H₂O.

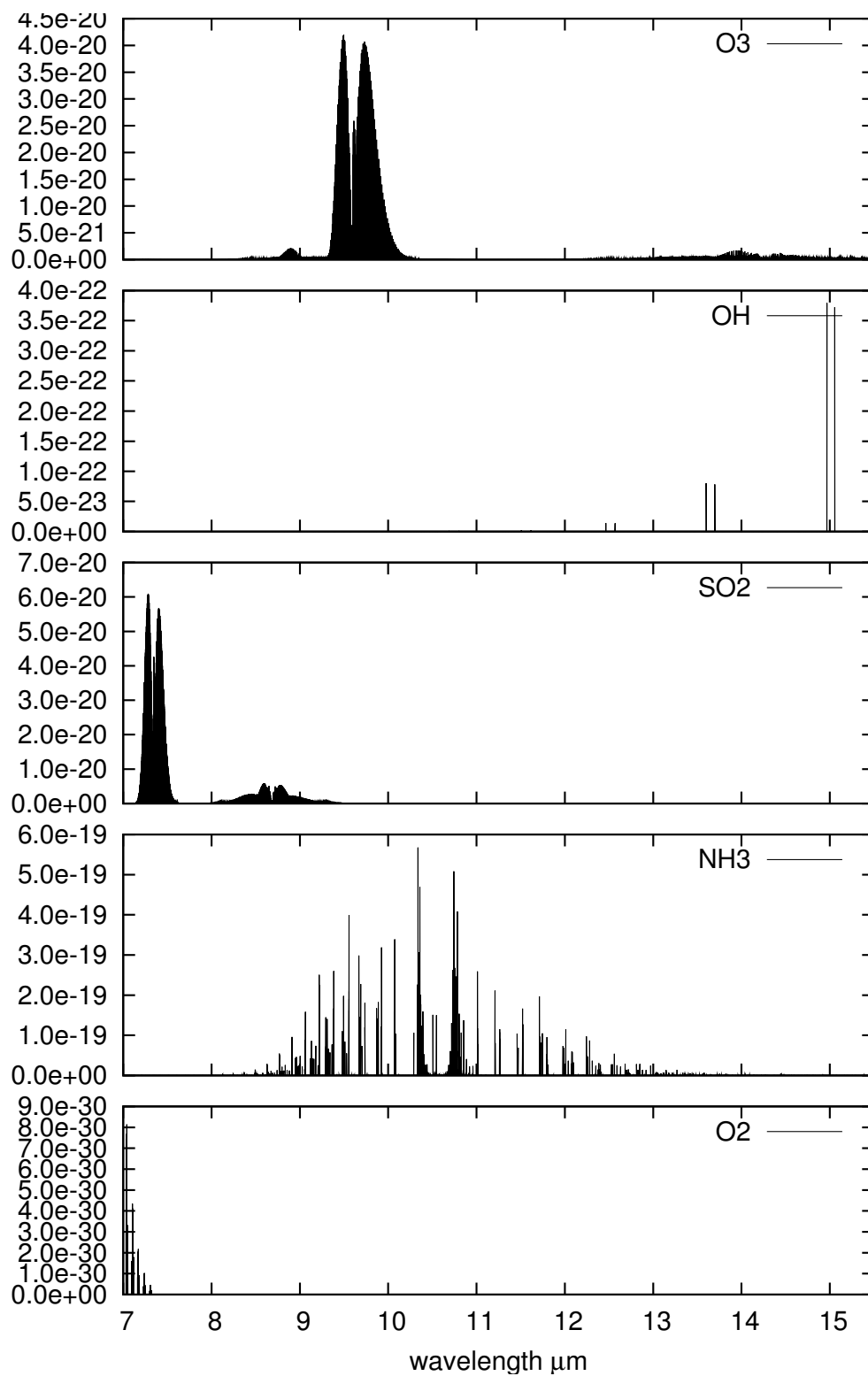


FIG. 13: HITRAN line locations and line strengths in units of $\text{cm}^{-1}/\text{molecule cm}^{-2}$ for O₃, OH, SO₂, NH₃ and O₂.

Appendix E: Software Problem Reports

1. VLTSW20050024

Display VLT SPR VLTSW20050024 [Image] Help - [Image] Logout

Field Label Field Value
 Problem Number VLTSW20050024
 Originator ssandroc
 Location ESO Paranal
 Type change request
 Create-date 2005/01/25 16:50:54
 Responsible vltsccm
 Package TCS Telescope Control System (kwirenst gchiozzi awalland rkarban)

Priority
 Status open

Closed Status
 Module Name tcs
 Module Version 1.147

cc rkarban jargomed jsyromi

Synopsis GPS + geographical positions

cc filter rkarban jargomed jsyromi

Description The geographical positions used by TCS should be updated. Based on the GPS timeserver values as input, the following table can be calculated. Compared to the previous values (taken from the VLT whitebook) the difference is about +6.5 arcsec (or 200 m) in both directions.

GPS-Timeserver:

Longitude Latitude
 d m s rad d m s rad
 TS 70 24 18.948 1.228803656 -24 37 41.634 -0.429843732

Unit Telescopes:

Longitude Latitude
 d m s rad d m s rad
 UT1 70 24 18.27 1.228800386 -24 37 39.44 -0.429833092
 UT2 70 24 17.39 1.228796107 -24 37 37.80 -0.429825122
 UT3 70 24 16.32 1.228790929 -24 37 36.64 -0.429819523
 UT4 70 24 14.25 1.228780856 -24 37 37.36 -0.429823005

Auxiliary Telescope Stations:

Longitude Latitude
 d m s rad d m s rad
 A0 70 24 18.44 1.228801200 -24 37 40.59 -0.429838653
 A1 70 24 18.26 1.228800303 -24 37 41.08 -0.429841025
 B0 70 24 18.17 1.228799896 -24 37 40.50 -0.429838245
 B1 70 24 17.99 1.228798998 -24 37 40.99 -0.429840617
 B2 70 24 17.89 1.228798549 -24 37 41.24 -0.429841803
 B3 70 24 17.80 1.228798100 -24 37 41.48 -0.429842989
 B4 70 24 17.71 1.228797651 -24 37 41.73 -0.429844175
 B5 70 24 17.62 1.228797202 -24 37 41.97 -0.429845361
 C0 70 24 17.90 1.228798591 -24 37 40.42 -0.429837837
 C1 70 24 17.72 1.228797693 -24 37 40.91 -0.429840209
 C2 70 24 17.63 1.228797244 -24 37 41.15 -0.429841395
 C3 70 24 17.53 1.228796795 -24 37 41.40 -0.429842581
 D0 70 24 17.36 1.228795981 -24 37 40.25 -0.429837021
 D1 70 24 16.99 1.228794186 -24 37 41.23 -0.429841765
 D2 70 24 16.81 1.228793288 -24 37 41.72 -0.429844137
 E0 70 24 16.83 1.228793372 -24 37 40.08 -0.429836204
 G0 70 24 16.29 1.228790762 -24 37 39.91 -0.429835388
 G1 70 24 15.55 1.228787171 -24 37 41.87 -0.429844877
 G2 70 24 16.57 1.228792109 -24 37 39.18 -0.429831830
 H0 70 24 15.21 1.228785543 -24 37 39.58 -0.429833756
 I1 70 24 14.48 1.228781994 -24 37 40.72 -0.429839279
 J1 70 24 14.13 1.228780282 -24 37 40.06 -0.429836090
 J2 70 24 13.85 1.228778935 -24 37 40.79 -0.429839649
 J3 70 24 15.05 1.228784771 -24 37 37.61 -0.429824230
 J4 70 24 15.24 1.228785668 -24 37 37.12 -0.429821857
 J5 70 24 15.52 1.228787015 -24 37 36.39 -0.429818299
 J6 70 24 15.79 1.228788362 -24 37 35.65 -0.429814741
 K0 70 24 14.14 1.228780324 -24 37 39.24 -0.429832124
 L0 70 24 13.87 1.228779019 -24 37 39.16 -0.429831716
 M0 70 24 13.60 1.228777714 -24 37 39.07 -0.429831308

Worklog

Last-modified-by

Modified-date

Status History

Status Modified-Time Modified-By
 closed 2005/01/25 16:50:54 ssandroc

2/18/2005 8:39:16 PM ssandroc

tcs 1.148 contains the new positions for UT1-4 and an average for ATs; the exact AT station positions must still be updated in the ATCS SW.

3/8/2005 5:15:56 PM vltscm

assigned to SSA for JAN2006

3/20/2005 3:22:21 PM mathar

(i) I propose to change the sign of the longitudes to become compatible with the sign convention of ESO ISS GEOLON in the primary headers.

(ii) the nominal accuracy of $1.e-9$ rad would be about 6.38 mm (with an earth radius of about 6380 km). Since the daily tidal motion on Paranal is up to 1.5 cm in all three directions, it makes sense to record *when* these data have been taken for later reduction of the tidal effects. (I am not sure whether the actual accuracy, given finite sizes of any GPS antenna and the weather dependence of the GPS signal delays would warrant such a precaution.)

(iii) If this accuracy is maintained, I propose to define this as the mean center position in the middle of the M3 iron surface, since this seems to be the best definition of the baseline "anchor" point.

5/14/2006 12:37:03 AM ssandroc

Positions have meanwhile been implemented for UTs and ATs.

Note that λ used here has the opposite sign to what has been used in the SPR reproduced above.

2. VLTSW20050104

Problem Number VLTSW20050104

Create-date 3/2/05 11:03:41 AM

Module Name atcsmon

Module Version

Description update the position table according to measurements provided in VLTSW20050024

Worklog rkarban 7/27/05 11:04:58 AM
 done in atcsmon 1.32

mathar 6/15/05 3:05:49 PM

Are the latitudes meant to be geodetic or geocentric?

I see that tcs/src/tcsVcc.c uses slaAoppa() in tcsCoord2AltAz(), which is defined to be fed with geodetic angles; it does the parallax calculation internally with some mean 1/298 prolate earth. From there I'd deduce that the tcs/dbl values are geodetic, but I cannot find any specific documentation, neither in the white book nor in the tcs module, nor in VLTSW20000166.

For Paranal, the difference between the two angles is about $695'' * \sin(2 * \phi)$, or 530 arcsec at $\phi = -0.4298$ rad.

vltscm 4/1/05 6:38:45 PM

assigned to RKA for OCT2005

Status closed

Closed Status solved

3. VLTSW20060050

Problem Number VLTSW20060050

Create-date 2/14/06 6:26:32 PM

Module Name issarray, dicISS

Module Version

Description The reference longitude/latitude defined in ISS database shall refer to UVW=0 (between UT1 and UT2).
 SPR VLTSW20050024 defines new values for all stations.
 From these data the correct longitude and latitude can be computed as

1.228798831 -0.429829904 (radians)

The issarray class file shall be updated accordingly

The ISS dictionary shall be updated to give 8 decimal resolution (degrees). The comment shall clarify the reference point.

Worklog vltscm 2/24/06 2:21:29 PM

assigned to AWA - closed as solved

awalland 2/15/06 5:39:37 PM
 Updated in issarray v 4.11.
 Tested OK in CM.
 Can be closed after assignment.

Status closed
 Closed Status solved

4. VLTSW20060066

From ARSystem@eso.org Wed Jul 26 16:09:49 2006
 Date: Wed, 26 Jul 2006 16:03:00 +0200 (MEST)
 From: ARSystem <ARSystem@eso.org>
 Reply-To: ARSystem <ARSystem@eso.org>
 To: mathar@strw.leidenuniv.nl
 Subject: VLTSW20060066 closed

The problem VLTSW20060066 has been closed

Problem Number : VLTSW20060066
 Originator : mathar
 Responsible : awalland
 Status : closed
 Package : VLTI-ISS (awalland nhouse)
 Module Name : isstrkws
 Module Version : 3.4
 Type : sw error
 Location : Leiden Observatory
 Closed Status : solved
 cc : pgitton,ott@four-d.de,ipercher,Gilles.Duvert@obs.ujf-grenoble.fr
 Synopsis : unexpected values of ISS PBLAij
 Description : The calculation of PBLAij in the isstrkws seems to be either in error
 or poorly documented. The actual calculation projects the straight
 projected baseline vector (difference between the baseline vector and
 the delay vector into the star direction) onto the UV coordinate system
 and calculates some sort of azimuth angle (w.r.t. the horizontal
 West-South coordinate system). Most people in the interferometric community
 would expect to get the position angle discussed
 in section IIC of
<http://www.strw.leidenuniv.nl/~mathar/public/matharMIDI20051110.pdf>
 Worklog :
 02/27/06 18:35:51 awalland
 The PBLAij has been implemented according to SPR VLTSW20040333.
 This SPR has been triggered by AMBER consortia and no complains have been raised
 after this implementation. Please consult AMBER consortia and agree on a different
 algorithm if that is required.
 The algorithm is given by Philippe Gitton and reproduced below.

Calculation of the angle between the projected baseline vector wrt North direction
 =====
 GIP - May 10, 2005

The reference frame used is defined as
 * -> X along East
 * -> Y along North
 * -> Z along Zenith

Let's define two vectors:

Unit vector star defining the direction in which the telescopes point at
 using VLT convention:
 AZ = 0 when pointing south
 AZ = 90 when pointing east

```
star[0] = sin(az)*cos(alt);
star[1] = -cos(az) *cos(alt);
star[2] = sin(alt);
```

```
/* Baseline vector from TEL 1 to TEL 2 in units of meters */
baseline[0] = coordTEL2[0] - coordTEL1[0];
baseline[1] = coordTEL2[1] - coordTEL1[1];
baseline[2] = coordTEL2[2] - coordTEL1[2];
```

```
/* The sidereal OPD (sign being either positive or negative) is computed via: */
```

```

sidOPD = star[0]*baseline[0]+star[1]*baseline[1]+star[2]*baseline[2];

/* The projected baseline vector ProjBaseline in meters is: */
ProjBaseline[0] = baseline[0] - sidOPD x star[0];
ProjBaseline[1] = baseline[1] - sidOPD x star[1];
ProjBaseline[2] = baseline[2] - sidOPD x star[2];

/* Angle theta from North to the projection in the North-East plane of the projected baseline
   angle = 0 if projection along North
   angle = 90 deg if angle along East */

theta = arctan(ProjBaseline[0]/ProjBaseline[1]);

```

03/03/06 15:54:16 mathar

The OIFITS data format explicitly specifies the direction of the (x,y) plane-- and therefore the (u,v) plane--that catches the wavefront: this plane is orthogonal to the direction of propagation, *not* orthogonal to the topocentric zenith direction. To get a correct representation of the coordinates as $x=\cos(\text{angle})\cdot\text{PBL}$, $y=\sin(\text{angle})\cdot\text{PBL}$ in OI_VIS tables [or angle replaced by angle+180 or angle+90 which is not explicitly defined by OIFITS], the software must absolutely *avoid* to set angle=PBLA as currently provided.

Note also that the angle is not defined modulo 180 [as currently implemented with the arctan()] but modulo 360 degrees, as implemented with an arctan2(). This is because the first and the second telescope define a baseline vector, and the projected baseline vector switches direction if these are swapped. This adds 180 degrees to the angle that ought be computed, and is equivalent to a sign convention for OPD's. [This is independent of the obscure "wall-based" sign convention used within the VLTI software.]

Note in passing that the ARRAY[XYZ] values in the ARRAY_GEOMETRY table produced by ISS are also not compatible with the OIFITS standard: according to OI_FITS the X component would be the value projected to the Greenwich meridian, and the Y component form a right-handed coordinate system with the Z component where Z points to the North. So for Paranal at -70 deg of longitude as in ESO ISS GEOLON (although some astronomers would wrongly argue this is +70 deg) we would need ARRAYX>0 and ARRAYY<0 and |ARRAYX|<|ARRAYY| to be compatible with OIFITS.

03/30/06 22:41:48 mathar

From Fabien.Malbet@obs.ujf-grenoble.fr Mon Feb 27 22:29:53 2006
Return-Path: <Fabien.Malbet@obs.ujf-grenoble.fr>
Date: Mon, 27 Feb 2006 22:29:35 +0100
From: Fabien Malbet <Fabien.Malbet@obs.ujf-grenoble.fr>
To: Richard Mathar <mathar@strw.leidenuniv.nl>
CC: Gerard Zins <gerard.zins@obs.ujf-grenoble.fr>, Gilles Duvert <Gilles.Duvert@obs.ujf-grenoble.fr>
Subject: Re: Fwd: Remarks added to VLTSW20060066

Dear Richard,

I have forwarded your request to our software team. Can you tell us a little bit more about the conventions you are using? I am in vacation riught now and I cannot check but we try to comply with usual conventions of optical and radio interferometry. Hopefully, Gilles Duvert will be able to reply to you on this subject.

Cheers,
fabien.

From Gerard.Zins@obs.ujf-grenoble.fr Tue Feb 28 08:54:18 2006
Date: Tue, 28 Feb 2006 08:53:18 +0100
From: Gerard Zins <Gerard.Zins@obs.ujf-grenoble.fr>
To: Richard Mathar <mathar@strw.leidenuniv.nl>
CC: Fabien Malbet <Fabien.Malbet@obs.ujf-grenoble.fr>, Gilles Duvert <Gilles.Duvert@obs.ujf-grenoble.fr>
Subject: Re: [Fwd: Fwd: Remarks added to VLTSW20060066]

Dear Richard,

Gilles is in vacation this week. I will discuss this point with him next week, and we will keep you informed.

Best regards,

Gerard.

04/05/06 18:44:59 mathar

The computational steps towards the baseline orientation angle are, following the first proposal of Section IIC of my reference given before :
1) Compute A, the star azimuth, which is zero if the star is geographically South, +90 deg if the star is West of the observatory. This is equivalent to ISS AZ.

- 2) Compute A_b, the baseline azimuth on the platform. This is the time-independent azimuth of Tj in coordinates centered at Ti. It is zero if Tj is south of Ti, +90 deg if Tj is West of Ti. This angle is approximately 180 degrees plus what is tabulated in <http://www.eso.org/observing/etc/doc/vlti/baseline/baselinedata.txt>. [We use only the difference between A_b and A below, so both angles may be redefined with a different origin, for example a North=0 convention. The common sense of orientation is mandatory, though.] Depending on the local programming conventions, this is some atan2() of the telescope coordinate differences North/South and East/West.
- 3) Compute/Get the star elevation above the horizon, a=90 deg minus z, where z is the star azimuth. This is equivalent to ISS ALT.
- 4) Compute the auxiliary angle psi, in C notation psi=atan2(sinpsi,cospsi), from the 2 intermediate variables sinpsi=sin(A_b-A) and cospsi=cos(A_b-A)*sin(a) ... of course using radians instead of degrees. This implements Eqs. (35) and (36) of the current version of the reference.
- 5) Compute the parallactic angle p in the standard convention (that is zenith angle North-over-East): Imagine the star, the zenith Z and the north celestial pole (NCP) marked on the celestial sphere. Define the line from the observer to the star as an axis of rotation. Rotation of the NCP by the angle p around the axis moves the NCP onto the great circle defined by Z and the star. Since this angle is defined "North-over-East", one needs a left-handed sign convention with the aforementioned axis. [We avoid a clockwise or counter-clockwise terminology here because this depends on whether one looks at the celestial sphere from the inside or from the outside. It is impossible to tell from the current definition within DIC.ISS whether this is ISS PARANG as currently implemented.]
- 6) Compute the final angle p_i=p+psi+180 deg and normalize to the range 0..360 deg. p_i = slaDransrm(p+psi+M_PI)*DRAD2DEG
Use this as the header keyword.

There has been no statement on this subject by the AMBER team so far. The update of the keyword description on PLBAij in the DIC.ISS would simply be

comment: projected baseline orientation angle
description:

Let the projected baseline be the great semicircle on the celestial sphere that starts at T1, passes by the star, and ends at T2. Let a rotation axis point from the observer at the sphere center to the star. The keyword value is the angle that actively rotates the North Celestial Pole around this axis until it meets the semicircle. The sign of the angle is "North-over-East" as if one would impose a "left-handed" rule on this directed axis of rotation.

If, however, for historical reasons, anybody wants to keep the old computation of the keyword, the DIC.ISS needs a much more precise definition of the current implementation for the current PBLAij. Keep in mind that this information will be used by people who have neither access to the ESO SPR system to look up the Gitton proposal nor access to the source code of the isstrkws CMM module:

comment : topocentric doubly projected baseline angle
description:

Define a projected baseline vector vec(P) from the delay vector vec(D), which points into the star direction, and the baseline vector vec(Ti->Tj): vec(D)+vec(P)=vec(Ti->Tj). Project vec(P) on the topocentric plane defined by the observatory's horizon (ie, subtract its zenith component). The keyword value is some compass rose (=geographical) orientation, confined to the range [-90..90] degrees which means dropping this doubly projected baseline vector's sense of orientation.

Then, a new keyword for the standard projected baseline angle, like PBOAij, (short for projected baseline orientation angle from i to j) needs to be defined that is computed according to 1)-6), and gets the ESO-VLT-DIC.ISS description mentioned first.

04/10/06 17:54:07 vltscmm
SPR assigned to AWA for JULY 2006
07/13/06 14:57:15 awalland

The new algorithm has been implemented in test program isstestPBLA.c available in isstest v 1.45. Test cases have been defined, documented and verified (isstestPBLA.doc) DMD has confirmed they have no objections to this change (no side effect on official MIDI and AMBER pipeline).

Next steps

- change the algorithm in isstrkws (Juergen)

- update documentation in dicISS (Anders)

For clarity the final algorithm is reproduced below:

```
double pblaRMA (double alt, double az, double prltic, double T1[3], double T2[3])
{
    vltDOUBLE      a, A, A_b, p;
    vltDOUBLE      sinpsi, cospsi, psi;

    double         rma;

    /*
     * 1. Compute A, star azimuth, with FITS convention; 0=south, +90 west
     *    VLT convention is 0=south, +90 east
     */
    A = (360 - az) * DDEG2RAD;

    /*
     * 2. Compute baseline azimuth on the platform
     *    This is zero if T2 is south of T1 and +90 deg if T2 is west of T1.
     *    It seems that DLCS applies the convention X pos to west and Y pos to south
     *    for station coordinates (T vectors).
     *    In a south-over-west convention for 'A_b' and 'a', the y-component
     *    of the atan2(y,x) must represent +West and the x-component +South.
     *    The vector from T1[.] to T2[.] is obtained as T2[.]-T1[.].
     */
    A_b = atan2( (T2[0] - T1[0]), (T2[1] - T1[1]) );

    /*
     * 3. Get a, star elevation
     *    This is directly given by VLT altitude
     */
    a = alt * DDEG2RAD;

    /*
     * 4. Compute auxiliary angle psi
     */
    sinpsi = sin(A_b - A);
    cospsi = cos(A_b - A) * sin(a);
    psi = atan2(sinpsi,cospsi);

    /*
     * 5. Get parallactic angle.
     *    This value is computed by ISS using standard slaPa
     */
    p = prltic * DDEG2RAD;

    /*
     * 6. Compute final angle
     */
    rma = slaDranrm(p + psi + DPI) * DRAD2DEG;

    return rma;
}

```

07/17/06 10:38:19 jott

The modifications are implemented and archived in isstrkws v. 3.7. The tat test is extended to verify values given in isstest/src/isstestPBL

07/25/06 15:10:13 awalland

Description of keyword is updated in dicISS v 1.41.

07/26/06 16:02:48 awalland

Tested OK in control model.

Data in FITS header and isstest program consistent.

Configuration UT1 and UT4. DOUBLE value is azimuth expressed in VLT convention

```
HIERARCH ESO ISS ALT          =      65.190 / Altitude angles at start
HIERARCH ESO ISS PARANG START=     123.159 / Parallactic angle at start
HIERARCH ESO ISS PBLA12 START=      245.2 / Projected baseline orientation ang
HIERARCH ESO ISS PARANG END   =     123.159 / Parallactic angle at end
HIERARCH ESO ISS PBLA12 END   =      245.2 / Projected baseline orientation ang
DOUBLE value = 244.157236

```

```
isstestPBLA 65.190 244.157 123.159 -103.30582608 -43.9989351911 0 9.924885621 20.334616923 0
alt=65.19, az=244.16, prltic=123.16 T1: -103.306 -43.999 0.00, T2: 9.925 20.335 0.00
A 2.022, A_b 1.054, a 1.138, psi -0.82 0.51 -1.012, p 2.150
GIP pbla = 55.4 deg
RMA pbla = 245.2 deg

```

HIERARCH ESO ISS ALT = 58.385 / Altitude angles at start

```

HIERARCH ESO ISS PARANG START= 96.496 / Parallaxic angle at start
HIERARCH ESO ISS PBLA12 START= 252.3 / Projected baseline orientation ang
HIERARCH ESO ISS PARANG END = 96.496 / Parallaxic angle at end
HIERARCH ESO ISS PBLA12 END = 252.3 / Projected baseline orientation ang
DOUBLE value = 278.625846

```

```

isstestPBLA 58.385 278.626 96.496 -103.30582608 -43.9989351911 0 9.924885621 20.334616923 0
alt=58.38, az=278.63, prltic=96.50 T1: -103.306 -43.999 0.00, T2: 9.925 20.335 0.00
A 1.420, A_b 1.054, a 1.019, psi -0.36 0.80 -0.423, p 1.684
GIP pbla = 53.5 deg
RMA pbla = 252.3 deg

```

```

-----
HIERARCH ESO ISS ALT = 67.931 / Altitude angles at start
HIERARCH ESO ISS PARANG START= -93.566 / Parallaxic angle at start
HIERARCH ESO ISS PBLA12 START= 227.9 / Projected baseline orientation ang
HIERARCH ESO ISS PARANG END = -93.566 / Parallaxic angle at end
HIERARCH ESO ISS PBLA12 END = 227.9 / Projected baseline orientation ang
DOUBLE value = 83.160835

```

```

isstestPBLA 67.931 83.161 -93.566 -103.30582608 -43.9989351911 0 9.924885621 20.334616923 0
alt=67.93, az=83.16, prltic=-93.57 T1: -103.306 -43.999 0.00, T2: 9.925 20.335 0.00
A 4.832, A_b 1.054, a 1.186, psi 0.59 -0.75 2.469, p -1.633
GIP pbla = 56.2 deg
RMA pbla = 227.9 deg

```

```

-----
HIERARCH ESO ISS ALT = 56.530 / Altitude angles at start
HIERARCH ESO ISS PARANG START= -138.449 / Parallaxic angle at start
HIERARCH ESO ISS PBLA12 START= 237.7 / Projected baseline orientation ang
HIERARCH ESO ISS PARANG END = -138.449 / Parallaxic angle at end
HIERARCH ESO ISS PBLA12 END = 237.7 / Projected baseline orientation ang
DOUBLE value = 133.142878

```

```

isstestPBLA 56.530 133.143 -138.449 -103.30582608 -43.9989351911 0 9.924885621 20.334616923 0
alt=56.53, az=133.14, prltic=-138.45 T1: -103.306 -43.999 0.00, T2: 9.925 20.335 0.00
A 3.959, A_b 1.054, a 0.987, psi -0.23 -0.81 -2.861, p -2.416
GIP pbla = 65.9 deg
RMA pbla = 237.7 deg

```

SPR is closed as solved.

Create-date : 02/25/06 00:33:51

5. VLTSW20060227

Problem Number VLTSW20060227

Synopsis Use switchyard and not telescope type when determine scales

Originator awalland

Responsible awalland

Status progress

Package VLT-ISS (awalland nhousen)

Module Name ISS

Type change request

Closed Status

cc ott@four-d.de,rollfinke@four-d.de

Description In many places ISS performs different coordinate transformations depending if the beam passes through beam compressor or not. The current standard configurations are UT with BC, AT without. With PRIMA STS AT will also passes through BC. Sometimes exotic configurations breaking this rule are used.

It would be safer always to use the position of the switchyard to determine which coordinate transformation to do, and not rely on the telescope type.

Worklog mathar 9/19/06 11:00:41 AM

The field rotation also depends on whether the beams pass by the DDL or are moved on immediately to the instruments via the switchyard. Actually, the effects of DDL and beam compressor on the field rotation are expected to cancel. Also, since the STS on the UT's is (currently) designed with one mirror less than the STS for the AT's, there will still be an effect from the telescope type (beyond the well known effects depending on the position of the telescopes North or South of the DL etc, VLT-TRE-ESO-15000-3092). The field rotation will also depend on the positions of the derotators of the AT's; to make things more exciting, there are two of them, one per AT, and they will be positioned differently, either by intention or mistake. See section IIA in the report public/matharMIDI20051110.pdf in my home page.

vltscm 9/18/06 5:23:30 PM

Appendix F: Spheroidal Coordinates

The Earth ellipsoid defines a geocentric latitude ϕ' and geodetic latitude ϕ , the latter measured by intersection of the normal to the tangential plane with the equatorial plane [22].

The files <http://www.strw.leidenuniv.nl/~mathar/vlti/oiArray.fits>, <http://www.strw.leidenuniv.nl/~mathar/vlti/oiArray2.fits> and <http://www.strw.leidenuniv.nl/~mathar/vlti/oiArray3.fits> contain OIFITS implementations of the different interpretations of the angles of latitude listed in Sect. E1: `oiArray.fits` interprets them as geocentric ϕ' , `oiArray2.fits` and `oiArray3.fits` interpret them as geodetic ϕ . Each case, the construction finds the pair (x, z) on the geoid using the flattening and equatorial radius. Depending on which interpretation is taken, these two places are some kilometers apart measured in the Cartesian coordinate system. (This is already expected from multiplying the directional difference of $v = 524'' = 0.00254$ rad given in Sect. E2—inserting 0.4298 rad of Sect. E3 in [22, (10)]—by the Earth radius ρ_e which yields 16 km.) We then follow the direction given by either ϕ or ϕ' further outwards by $H = 2681$ m for each station as to include the mountain altitude and use this as the sum of the `ARRAYi` and `STAXYZ` coordinates. These station coordinates are necessarily distributed on a slightly curved surface, because no attempt has been made to re-arrange the heights above the geoid to obtain a flat plane that includes all the points. The difference between `oiArray2.fits` and `oiArray3.fits` is that `oiArray2.fits` uses the IERS values of geoid flattening and equatorial radius [25], whereas `oiArray3.fits` uses the WGS84 values [27], causing a relative shift of the telescope array by ≈ 40 cm.

If one inserts the angular coordinates $-24.6274394, -70.4049869$ of Sec. E3 into <http://maps.google.com>, using the `Satellite` option, one hits the Paranal platform with a precision of better than ≈ 30 m [6]. This means the two ways of interpreting the coordinates are consistent. Most likely, the google maps are using a WGS84 system, although it is difficult to find any documentation on this issue.

Another hint on that the geodetic interpretation is correct is given by reverse astrometry with `IPHASE` run over the file `d14UT4U4IP3-d13UT3U3IP1_20060412.dat` of the `vltipom` module, which contains delay data obtained with `MIDI+FINITO` for the U4–U3 baseline. (This pair of telescopes stretches best from North to South and is presumably most sensitive to relocation along the geographic latitude.) If one assumes the angle is of geodetic origin, the `iphase` input file is fed with `-24 37 33.12` in the `SITE` configuration and produces a zenith component (tilt) of the baseline of 15 mm; if one assumes the angle is of geocentric origin and converts it to `-24 46 24.76` before using it as a `SITE` parameter, the zenith component of the fit becomes 72 mm. (The difference of 57 mm is expected because the North-South component of the U3–U4 baseline is 22.1 m, which multiplied by $v = 0.0025$ rad induces a tilt of 56 mm.) If one assumes that the better fit is the one with the smaller inclination of the baseline vector in the topocentric horizontal system, the fit with 15 mm and therefore the geodetic interpretation are preferred.

No response has been received from ESO on the question which of the two interpretations is correct.

Appendix G: Web Page Change Requests

1. WWW-31864

Your support request number WWW-31864 has now been closed. You will find the resolution at the END of this message.

Please contact us again quoting the above number should you find the resolution unsatisfactory.

Rgds.
ESO Web Team

```

Entry-Id           : WWW-31864
First Name        : Email
Last Name         : User
Category          : Web Pages
Short-Description : broken links
Problem Description :
09/04/06 13:47:24 mathar
The links to
http://www.eso.org/observing/etc/doc/vlti/lengthdata.txt
and to
http://www.eso.org/observing/etc/doc/vlti/baselinedata.txt
and to
http://www.eso.org/observing/etc/doc/vlti/posangledata.txt
at the bottom of
http://www.eso.org/observing/etc/doc/vlti/vltistations.html
are broken.
```

Richard J. Mathar, mathar@strw.leidenuniv.nl
 Server/Cluster : Observing
 Resolution :
 09/04/06 15:12:47 mnaumann
 Dear Richard,

many thanks for reporting these broken links. I've forwarded your report to the ETC webteam and they will contact you as soon as possible.

Kind regards,
 Michael

--

Michael Naumann * ESO, Karl Schwarzschild Str.2 85748 Garching
 Michael.Naumann@eso.org * <http://www.eso.org/mnaumann>
 ESO Webmaster * Tel/Fax +49 89 3200 6430, Germany

Appendix H: Acronyms

ARAL	Artificial Source and Alignment Toolkit
AT	Auxiliary Telescope (of the VLTI) http://www.eso.org/projects/vlti/AT/index_at.html
BC	Beam Combiner
BC	Beam Compressor
CMM	Configuration Management Module http://www.eso.org/projects/vlt/sw-dev/wwwdoc/dockit.html
DDL	Differential Delay Line http://www.mpia-hd.mpg.de/PRIMA-DDL/
DF	Dual Feed
DL	Delay Line
DLMT	Delay Line Mirror Translation Stage (of the MIDI warm optics)
ESO	European Southern Observatory http://www.eso.org
FINITO	Fringe-Tracking Facility of Nice and Torino
FITS	Flexible Image Transport System http://fits.gsfc.nasa.gov
fv	fits viewer http://heasarc.gsfc.nasa.gov/docs/software/ftools/fv/
GENIE	Ground based European Nulling Interferometry Experiment http://www.strw.leidenuniv.nl/~nevec/GENIE/
GUI	Graphical User Interface
IR	Infrared
ISAAC	Infrared Spectrometer and Array Camera http://www.eso.org/instruments/isaac/
ISS	Interferometric Supervisor-Software
IWS	Instrument Workstation
LST	Local sidereal time
MDL	main delay line http://www.eso.org/outreach/press-rel/pr-2000/phot-26-00.html
MIA	MIDI Interactive Analysis http://www.strw.leidenuniv.nl/~koehler/MIDI/
MIDI	Mid-Infrared Interferometric Instrument http://www.mpia.de/MIDI
MPIA	Max-Planck Institut für Astronomie, Heidelberg http://www.mpia.de

OIFITS	Optical Interferometry FITS Exchange Format http://www.mrao.cam.ac.uk/~jsy1001/exchange/
OPD	optical path difference
OPL	optical path length
OS	Observation Software
P2PP	Phase 2 Proposal Preparation http://www.eso.org/observing/p2pp
PRIMA	Phase-Reference Imaging and Microarcsecond Astrometry http://obswww.unige.ch/Instruments/PRIMA
PSF	point spread function
SF	Single Feed
SPR	Software Problem Report http://www.eso.org/vlt/sw-dev
STS	star separator
SWY	switchyard (table in the VLTI lab)
TAD	transverse atmospheric dispersion
URL	Universal Resource Locator
UT	Unit Telescope (of the VLTI) http://www.eso.org/projects/vlt/unit-tel/
VINCI	VLT Interferometer Commissioning Instrument
VLTI	Very Large Telescope Interferometer http://www.eso.org/vlti
ZOPD	zero OPD

Appendix I: Notations

α	right ascension
a, a'	star elevation; inclination of projected baseline plane towards horizontal
$A, \Delta A; A_b; A_\lambda$	star azimuth angle, and its change; baseline azimuth; visibility amplitude
b, \mathbf{b}_{12}	baseline length and vector
d	aperture diameter
δ	declination
D, D_a, D_i	OPD
e	eccentricity of the Earth geoid
f	Earth flattening factor
ϕ, ϕ'	field rotation angle, geographic latitudes
Φ	geographic latitude
φ	angular phase shift
h	hour angle, see page 9
H	observatory sea level altitude
L	path length
λ	wavelength; geographic longitude
p	parallactic angle
p_b	positional angle of the projected baseline circle
P	projected baseline
R	angular difference between true and apparent azimuth by TAD
ρ, ρ_e, ρ_p	Earth radius (equatorial and polar)
\mathbf{s}	unit vector into star direction
σ	wave-number $1/\lambda$
θ	angular separation between pointing and baseline vector
t	time
τ	baseline position angle
v	angle between geodetic and geocentric angles of latitude
U, V, W	Paranal Cartesian coordinates
ψ	intersection angle between projected baseline circle and star meridian
x, y	Cartesian components in a cut through the Earth geoid
$z, \Delta z$	zenith angle, differential zenith angle
Z	baseline angle seen from the Earth center

-
- [1] Ballester, P., and C. Sabet, 2002, *VLT Interferometer VLTI Data Interface Control Document*, VLT-SPE-ESO-15000-2764.
- [2] Boden, A. F., 2000, in *Principles of Long Baseline Stellar Interferometry*, edited by P. R. Lawson (National Aeronautics and Space Administration), p. 9, JPL publication 00-009 07/00.
- [3] Calabretta, M. R., and E. W. Greisen, 2002, *Astron. & Astrophys.* **395**, 1077.
- [4] Cox, A. N. (ed.), 2000, *Allen's Astrophysical Quantities* (Springer, Heidelberg), 4th edition.
- [5] Davis, J., and A. Richichi, 2003, *The Spectral Sensitivity Curve and Effective Wavelength for the VLTI with VINCI*, VLT-TRE-ESO-15810-3033.
- [6] Duvert, G., 2007, priv. commun.
- [7] Galliano, E., M. Schöller, M. Fischer, C. Hummel, S. Morel, F. Rantakyro, and M. Vannier, 2004, in *New Frontiers in Stellar Interferometry*, edited by W. A. Traub (Int. Soc. Optical Engineering), volume 5491 of *Proc. SPIE*, pp. 1540–1548.
- [8] Gandhi, P., C. S. Crawford, and A. C. Fabian, 2002, *Month. Not. Roy. Astron. Soc.* **337**(3), 781.
- [9] Gitton, P., 2003, Re: north angle, priv. commun.
- [10] Gitton, P., 2006, Re: VLT ICD question, priv. commun.
- [11] Gitton, P., R. Wilhelm, A. Glindemann, and F. Paresce, 2003, *Determination of the field and pupil rotation in the VLTI laboratory*, VLT-TRE-ESO-15000-3092.
- [12] Glazenborg, A., 2002, *MIDI Optical Design of the Cold Bench*, VLT-SPE-MID-15821-0101.
- [13] Jaffe, W. J., 2004, in *Astronomical Telescopes and Instrumentation*, edited by W. A. Traub (Int. Soc. Optical Engineering), volume 5491 of *Proc. SPIE*, pp. 715–725.

- [14] Leinert, C., 2003, Transfer of V, W -“field” onto MIDI, priv. commun.
- [15] Lord, S. D., 1992, *A New software tool for computing earth’s atmospheric transmission of near- and far-infrared radiation*, NASA Technical Memorandum 103957, NASA, URL <http://www.gemini.edu/sciops/ObsProcess/obsConstraints/ocTransSpectra.html>.
- [16] Mason, E., 2006, *Very Large Telescope, ISAAC User Manual*, VLT-MAN-ESO-14100-0841.
- [17] Mathar, R. J., 2004, arXiv:astro-ph/0411384 .
- [18] Mathar, R. J., 2004, *MIDI Observation Software, User and Maintenance Manual*, VLT-TRE-MID-15824-0264.
- [19] Mathar, R. J., 2005, *Baltic Astronomy* **14**(2), 277.
- [20] Mathar, R. J., 2006, *PRIMA Non-Astrometric Modes, External Fringe Tracking for MIDI*, UL-ICD-DDL-15728-0009.
- [21] Mathar, R. J., 2006, arXiv:astro-ph/0608273 .
- [22] Mathar, R. J., 2007, arXiv:0711.0642 [math.MG] .
- [23] Mathar, R. J., 2008, *Serb. Astr. J.* **177**, 115, E: the sine in the equation on the second line of p 117 should be squared.
- [24] Mathar, R. J., 2009, arXiv:0906.2575 [astro-ph.IM] .
- [25] McCarthy, D. D., and G. Petit, 2003, *IERS Technical Note No 32*, Technical Report, IERS Convention Centre, URL <http://www.iers.org/iers/publications/tn/tn32/>.
- [26] Menardi, S., 2000, *Interferometric Laboratory, Optical Layout*, VLT-DWG-ESO-15000-1738.
- [27] National Imagery and Mapping Agency, 2000, *Department Of Defense World Geodetic System 1984*, Technical Report TR8350.2, NIMA, URL <http://earth-info.nga.mil/GandG/publications/tr8350.2/tr8350.2.html>.
- [28] Pauls, T. A., J. S. Young, W. D. Cotton, and J. D. Monnier, 2004, in *New Frontiers in Stellar Interferometry*, edited by W. A. Traub (Int. Soc. Optical Engineering), volume 5491 of *Proc. SPIE*, pp. 1231–1239.
- [29] Pauls, T. A., J. S. Young, W. D. Cotton, and J. D. Monnier, 2005, *Publ. Astron. Soc. Pac.* **117**(837), 1255.
- [30] Pel, J.-W., 1999, *MIDI Preliminary alignment plan*, VLT-TRE-MID-15821-0107.
- [31] Puech, F., and P. Gitton, 2005, *Interface Control Document between VLTI and its Instruments*, VLT-ICD-ESO-15000-1826. On page 110, f_c^{-2} should read $f_c^{-8/3}$, $f < f$ should read $f < f_c$, and $1.38 \cdot 10^{-3}$ should read 1.38×10^{-3} .
- [32] Rivinius, T., and S. Morel, 2008, *MIDI User Manual*, VLT-MAN-ESO-15820-3519.
- [33] Rothman, L. S., D. Jacquemart, A. Barbe, D. C. Benner, M. Birk, L. R. Brown, M. R. Carleer, C. Chackerian Jr., K. Chance, L. H. Coudert, V. Dana, V. M. Devi, *et al.*, 2005, *J. Quant. Spectrosc. Radiat. Transfer* **96**, 139.
- [34] Smart, W. M., 1949, *Text-book on Spherical Astronomy* (Cambridge University Press, Cambridge), 4th edition.
- [35] Soler, T., 1998, *J. Geod.* **72**, 482.
- [36] Stanghellini, S., and A. Michel, 1998, *The Messenger* **94**, 10.
- [37] Tristram, K., 2007, *Mid-infrared interferometry of nearby Active Galactic Nuclei*, Ph.D. thesis, University of Heidelberg, URL <http://www.ub.uni-heidelberg.de/archiv/7525>.
- [38] Tubbs, R. N., and R. J. Mathar, 2006, *Astrometric Survey for Extra-Solar Planets with PRIMA, Astrometric Error Budget*, VLT-TRE-AOS-15753-0001 in the version of Dec. 2006.
- [39] Wallander, A., 2006, *ICD between VLTI Supervisor SW and VLTI Instrumentation SW*, VLT-ICD-ESO-15410-2117.
- [40] Wilhelm, R., B. Koehler, and P. Gitton, 2002, *Functional Description of the VLTI*, VLT-ICD-ESO-15000-1918. The radii of curvature of M2, M5 and M7 in Table 4-1 are wrong. See [36] for M2.
- [41] Young, J. S., W. D. Cotton, W. Gässler, R. Millan-Gabet, J. D. Monnier, T. A. Pauls, and I. Percheron, 2008 (Int. Soc. Optical Engineering), volume 7013 of *Proc. SPIE*, p. 70134H.